A Mathematical Model for Wideband Ranging

Stefania Bartoletti, *Student Member, IEEE*, Wenhan Dai, *Student Member, IEEE*, Andrea Conti, *Senior Member, IEEE*, and Moe Z. Win, *Fellow, IEEE*

***Abstract*—Wideband ranging is essential for numerous emerging applications that rely on accurate location awareness. The quality of range information, which depends on network intrinsic properties and signal processing techniques, affects the localization accuracy. A popular class of ranging techniques is based on energy detection owing to its low-complexity implementation. This paper establishes a tractable model for the range information as a function of wireless environment, signal features, and energy detection techniques. Such a model serves as a cornerstone for the design and analysis of wideband ranging systems. Based on the proposed model, we develop practical soft-decision and hard-decision algorithms. A case study for ranging and localization systems operating in a wireless environment is presented. Sample-level simulations validate our theoretical results.**

***Index Terms*—Network localization, wideband ranging, energy detection, range likelihood, TOA estimation.**

I. Introduction

WIDEBAND RANGING is a key enabler for emerging applications, such as logistic, safety, security, and military, relying on accurate location awareness [1]–[9]. The localization accuracy of navigation and radar systems is affected by the quality of range information [10]–[19]. Range information such as range likelihood or range estimate can be extracted from the received signals for soft-decision or hard-decision localization, respectively [20]–[22]. The quality of range information depends on network intrinsic properties and signal processing techniques [23]–[29].

The design and analysis of ranging systems require models for describing range information as a function of the propagation environment, signal features, and detection techniques. A popular class of ranging techniques is based on energy detection, which determines the absence or presence of signals based on the level of energy collected over certain observation intervals [30]. The energy detectors (EDs) have been employed in many contexts, including range estimation in positioning systems [31]–[33], spectrum sensing in cognitive radios [34]–[36], and carrier sensing in network access protocols [37]–[39] owing to their low-complexity implementation. Energy detection was introduced in [30] to detect unknown deterministic signals in additive white Gaussian noise (AWGN) channels. More recently, the analysis has been extended to detection of random signals in AWGN channels [40]–[43], random signals in flat fading channels [44]–[46], and deterministic signals in the presence of interference [47]–[49].

Classical ranging techniques based on energy detection provide hard-decision range estimates that are consonant with the time-of-arrival (TOA) of the received signals. The lack of accurate models for range estimates in wireless propagation environments[1] coerces the design of EDs to consider simplified assumptions such as AWGN channels. Such assumptions do not account for multipath fading or obstructed propagation, leading to inaccurate ranging in wireless environments.

In this paper, we derive a mathematical model that describes the range information by providing range likelihood and range estimate for soft-decision and hard-decision localization, respectively. The goal is to establish a range information model that accounts for the wireless environment and signal features to facilitate the design and analysis of optimal EDs. The key contributions of the paper are as follows:

- Derivation of a range information model for design and analysis of wideband ranging systems based on energy detection;
- Development of low-complexity ranging algorithms with optimal EDs for soft-decision and hard-decision localization;
- Quantification of the benefits to location awareness provided by the proposed range information model in wireless environments.

The remainder of the paper is organized as follows. Section II presents the ranging system and the energy samples distribution. The range information model for soft-decision and hard-decision algorithms is developed in Section III. Section IV presents a tractable range information model for wideband systems. Section V provides guidelines for the design of ED for location-aware networks based on the proposed models. Section VI describes a case study for ranging and localization. Finally, conclusions are given in Section VII.

Notation: For a random variable (RV) X, the x, $f_{\mathsf{X}}(\cdot)$, and $F_{\mathsf{X}}(\cdot)$ denote its realization, distribution function, and cumulative distribution function (CDF), respectively. Let

Manuscript received March 15, 2014; revised September 06, 2014; accepted October 13, 2014. Date of publication November 13, 2014; date of current version February 11, 2015. This work was supported in part by the Italian MIUR project GRETA under Grant 2010WHY5PR, the Office of Naval Research under Grant N00014-11-1-0397, the Defense University Research Instrumentation Program under Grant N00014-08-1-0826, the Copernicus Fellowship, and the MIT Institute for Soldier Nanotechnologies. The guest editor coordinating the review of this manuscript and approving it for publication was Prof. Pramod Varshney.

S. Bartoletti and A. Conti are with ENDIF, University of Ferrara, 44100 Ferrara, Italy (e-mail: stefania.bartoletti@unife.it; a.conti@ieee.org).

W. Dai and M. Z. Win are with LIDS, Massachusetts Institute of Technology, Cambridge, MA 02139 USA (e-mail: whdai@mit.edu; moewin@mit.edu).

Color versions of one or more of the figures in this paper are available online at http://ieeexplore.ieee.org.

Digital Object Identifier 10.1109/JSTSP.2014.2370934

[1]The range estimate is often modeled as a Gaussian random variable [50]–[53].

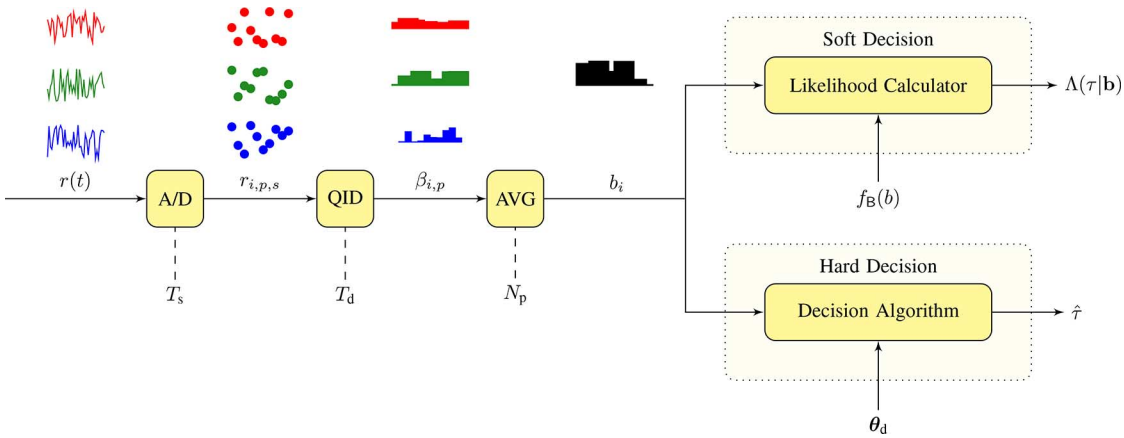

Fig. 1. Soft-decision and hard-decision energy detection system.

$\mathsf{X} \sim \mathcal{N}(\mu, \sigma^2)$ denote a Gaussian distributed RV with mean μ and variance σ^2. Let $\phi(\cdot)$ and $\Phi(\cdot)$ denote the probability distribution function (PDF) and CDF of a standard Gaussian RV, respectively. The symbol $\lfloor x \rfloor$ denotes the largest integer less than or equal to x. Let $\mathbf{0}$ be the all-zero vector. The notation $\mathcal{E}^{\mathrm{c}}$ denotes the complement of an event $\mathcal{E}$.

II. Ranging System

This section describes the energy detection principle and formulates the statistical model for the energy samples at the ED's output.

A. Energy Detection

Consider a ranging system composed of a transmitter at position $\mathbf{p}_{\mathrm{t}}$ that emits N_{p} copies of a signal $s(t)$ with repetition period T_{p}, and a receiver at position $\mathbf{p}_{\mathrm{r}}$.[2] The aim of the ranging system is to detect the signal $s(t)$ and to estimate its TOA τ with respect to a reference time t_0 from the received signal based on N_{p} observations each with duration T_{obs}.[3] The reference time t_0 can be the time at which the signal was transmitted (e.g., TOA-based localization or radar systems) or be the time shared among several receivers (e.g., time difference-of-arrival (TDOA)-based localization systems).

For ranging techniques based on energy detection, energy samples (namely energy bins) are collected, one for each dwell time T_{d}. After band-pass filtering for noise reduction (and clutter mitigation in case of radar networks), the received waveforms are non-coherently accumulated for soft-decision and hard-decision processing as illustrated in Fig. 1. The received signal can be written as

$$r(t) = u(t) + n(t) \tag{1}$$

where $u(t)$ is the received probe signal after propagating through a wireless channel with impulse response $h(t;\varsigma)$ and $n(t)$ is the thermal noise component. The received probe signal is a sequence of channel responses to the transmitted signal replicas, the first of which can be written as

$$u(t) = \int h(t;\varsigma)\, s(t-\varsigma)\, d\varsigma. \tag{2}$$

The received signal is first sampled by an analog-to-digital (A/D) converter with sampling period T_{s}. At the sampling instant $t_{i,p,s} = i\,T_{\mathrm{d}} + p\,T_{\mathrm{p}} + s\,T_{\mathrm{s}}$, with $i = 0, 1, \ldots, N_{\mathrm{b}} - 1$ and $p = 0, 1, \ldots, N_{\mathrm{p}} - 1$, the sample of the received signal is given by

$$r_{i,p,s} = r(t_{i,p,s}) = u_{i,p,s} + n_{i,p,s} \tag{3}$$

where $u_{i,p,s} = u(t_{i,p,s})$ and $n_{i,p,s} = n(t_{i,p,s})$. After A/D conversion, waveform samples are processed by a quadrature integrate and dump (QID) block that squares and integrates them over a dwell time T_{d} to obtain $N_{\mathrm{b}} = \lfloor T_{\mathrm{obs}}/T_{\mathrm{d}} \rfloor$ energy bins. The ith energy bin corresponding to the pth observation is given by

$$\beta_{i,p} = \sum_{s=0}^{N_{\mathrm{sb}}-1} r^2(t_{i,p,s}) = \sum_{s=0}^{N_{\mathrm{sb}}-1} (u_{i,p,s} + n_{i,p,s})^2 \tag{4}$$

where $N_{\mathrm{sb}} = \lfloor T_{\mathrm{d}}/T_{\mathrm{s}} \rfloor$ is the number of signal samples per bin. The energy bins obtained from each observation interval are processed by an averaging (AVG) block over the N_{p} observations as

$$b_i = \frac{1}{N_{\mathrm{p}}} \sum_{p=0}^{N_{\mathrm{p}}-1} \beta_{i,p} \tag{5}$$

resulting in a vector of energy bins $\mathbf{b} = [b_0, b_1, \ldots, b_{N_{\mathrm{b}}-1}]$. The vector of energy bins at the output of the ED is used as input for soft-decision or hard-decision processing.

The detection of the signal $s(t)$ and the estimation of its TOA τ are based on the energy bin vector $\mathbf{b}$. Classical approaches follow the Bayesian hypothesis testing, involving the comparison of the energy bins with a threshold. Such a threshold is often chosen to achieve a constant false-alarm rate resulting in a certain misdetection rate.

Typically, ranging is based on hard-decision algorithms which provide the TOA estimate from the observed energy

[2]Several techniques are available in the literature to estimate the repetition period of a signal when it is unknown, see e.g., [54].

[3]Range and TOA are used interchangeably throughout this paper since the former is a bijective function of the latter.

bins. If the distribution function of energy bins is known, then soft-decision algorithms can be conceived providing a posterior PDF of the TOA estimates. Models for soft-decision and hard-decision algorithms, which will be provided in Section III, depend on the distribution of the energy samples given in the following.

B. Energy Samples

Each element b_i of the vector $\mathbf{b}$ is an instantiation of the RV

$$\mathsf{B}_i = \sum_{s=0}^{N_{\rm sb}-1} \mathsf{X}_{N_{\rm p}}^{(i,s)} \tag{6}$$

where

$$\mathsf{X}_n^{(i,s)} = \frac{1}{n}\sum_{p=0}^{n-1}(\mathsf{U}_{i,p,s} + \mathsf{N}_{i,p,s})^2 \tag{7}$$

is the sample average, in p, of the energy bins. In particular, $\mathsf{U}_{i,p,s}$ and $\mathsf{N}_{i,p,s}$ are independent random samples of the received probe signal and of the thermal noise, respectively. Note that B_i depends on the transmitted signal, thermal noise, true TOA τ, wireless channel, and ED parameters. Let $\boldsymbol{\theta} = [\tau\ \boldsymbol{\theta}_{\rm h}\ \boldsymbol{\theta}_{\rm d}]$ where $\boldsymbol{\theta}_{\rm h}$ and $\boldsymbol{\theta}_{\rm d}$ are the vectors of parameters representing the wireless channel and the ED, respectively. The normalized bin $\mathsf{B}_i N_{\rm p}/\sigma^2$ conditioned on $\boldsymbol{\theta}$ is distributed as a noncentral chi-squared RV with $N_{\rm p}N_{\rm sb}$ degrees of freedom, i.e.,

$$\mathsf{B}_i \frac{N_{\rm p}}{\sigma^2} \overset{|\boldsymbol{\theta}}{\sim} \chi^2_{N_{\rm p}N_{\rm sb}}(\lambda_i) \tag{8}$$

where λ_i is the noncentrality parameter, which depends on $\boldsymbol{\theta}$, given by [30]

$$\lambda_i = \sum_{p=0}^{N_{\rm p}-1}\sum_{s=0}^{N_{\rm sb}-1} \frac{u_{i,p,s}^2}{\sigma^2} \tag{9}$$

with $u_{i,p,s}$ denoting the instantiation of the RV $\mathsf{U}_{i,p,s}$ and σ^2 denoting the variance of the zero-mean thermal noise. Therefore,

$$f_{\mathsf{B}_i}(b|\boldsymbol{\theta}) = \frac{N_{\rm p}}{2\sigma^2} e^{-\frac{bN_{\rm p}+\lambda_i\sigma^2}{2\sigma^2}} \left(\frac{bN_{\rm p}}{\lambda_i\sigma^2}\right)^{\frac{N_{\rm p}N_{\rm sb}-2}{4}} I_{\frac{N_{\rm p}N_{\rm sb}-2}{2}}\left(\sqrt{\frac{\lambda_i b N_{\rm p}}{\sigma^2}}\right) \tag{10a}$$

$$F_{\mathsf{B}_i}(b|\boldsymbol{\theta}) = e^{-\frac{\lambda_i}{2}} \sum_{r=0}^{+\infty} \frac{(\lambda_i/2)^r}{r!} \frac{\gamma\left(\frac{N_{\rm p}N_{\rm sb}}{2}+r, \frac{bN_{\rm p}}{2\sigma^2}\right)}{\Gamma\left(\frac{N_{\rm p}N_{\rm sb}}{2}+r\right)} \tag{10b}$$

where $I_a(\cdot)$ is the modified Bessel function of the first kind with order a, $\gamma(\cdot,\cdot)$ denotes the lower incomplete Gamma function, and $\Gamma(\cdot)$ denotes the Gamma function [55].

Remark 1: In practice, the noise variance can be estimated by observing the energy bins in an absence of the transmitted signal and each λ_i depends on the wireless channel instantiation. Therefore, the derivation of the range estimation error distribution requires averaging the conditional energy bin distribution over all possible wireless channel instantiations [20].

III. Range Information Model

This section offers the range information model by providing the range likelihood and the range estimate, as well as the range error.

A. Range Likelihood

The range likelihood function is determined from the observation b_i in (5) and the distribution of B_i for each energy bin, as shown in Fig. 1. The RVs B_i's are independent and non-identically distributed with noncentrality parameter depending on $\boldsymbol{\theta}$. The range likelihood function for a given bins observation can be written as

$$\Lambda(\varsigma|\mathbf{b}) = \prod_{i=0}^{N_{\rm b}-1} f_{\mathsf{B}_i}(b_i|\varsigma, \boldsymbol{\theta}_{\rm h}, \boldsymbol{\theta}_{\rm d}). \tag{11}$$

Remark 2: The range likelihood function can be used for both soft-decision and hard-decision localization. For soft-decision localization, a localization algorithm can directly process the likelihood functions obtained from one or more receivers to determine the position of a node. For hard-decision localization, a localization algorithm first obtains the TOA estimate by seeking a maximum of the range likelihood function, and then processes such estimates from one or more receivers to determine the position of a node.

B. Range Estimate

A widely used approach for ranging is based on hard-decision algorithms that aim to determine the index $\hat{\imath}$ of the first bin containing a portion of the transmitted signal energy. Therefore, the index $\hat{\imath}$ can be thought as the instantiation of a discrete RV I taking value in the set $\mathcal{B} = \{0, 1, \ldots, N_{\rm b}-1\}$.

Let the TOA estimate $\hat{\tau}$ be the instantiation of the RV T with PDF $f_{\mathsf{T}}(t|\boldsymbol{\theta})$.[4] The RV T depends on I since $\hat{\tau}$ is chosen from the interval $[\hat{\imath}\,T_{\rm d}, (\hat{\imath}+1)\,T_{\rm d})$. Consider a bijective function $\hat{\tau} = g(\hat{\imath})$, e.g., the TOA estimate is chosen to be the center of the interval as $g(\hat{\imath}) = \hat{\imath}\,T_{\rm d} + T_{\rm d}/2$. Therefore, the distribution function $f_{\mathsf{T}}(t|\boldsymbol{\theta})$ of the TOA estimate is determined by the distribution function $f_{\mathsf{I}}(i|\boldsymbol{\theta})$ of I. The $f_{\mathsf{T}}(t|\boldsymbol{\theta})$ depends on $\boldsymbol{\theta}$ since the RV I is a function of both the wireless channel and the ED.

Various hard-decision algorithms have been proposed in the literature [12], [20], [56]. This paper analyzes the most popular hard-decision algorithms: threshold crossing search (TCS), maximum bin search (MBS), jump back and search forward (JBSF), and serial backward search (SBS) algorithms. These algorithms involve the comparison of each bin value with a corresponding threshold. Let the threshold crossing event be $\mathcal{C}_{\rm th} = \{\exists i \in \mathcal{B} : \mathsf{B}_i > \xi_i\}$ where ξ_i is the threshold for the bin B_i for $i \in \mathcal{B}$. The probability mass function (PMF) of the selected bin index I conditioned on $\mathcal{C}_{\rm th}$ and $\boldsymbol{\theta}$ can be written as[5]

$$f_{\mathsf{I}}(i|\boldsymbol{\theta}) = \mathbb{P}\{\mathcal{S}_i \cap \mathcal{C}_{\rm th}|\boldsymbol{\theta}\}/\mathbb{P}\{\mathcal{C}_{\rm th}|\boldsymbol{\theta}\} \tag{12}$$

where the event $\mathcal{S}_i \cap \mathcal{C}_{\rm th}|\boldsymbol{\theta} = \{i \text{ is selected}, \mathcal{C}_{\rm th}|\boldsymbol{\theta}\}$ and

$$\mathbb{P}\{\mathcal{C}_{\rm th}|\boldsymbol{\theta}\} = 1 - \prod_{n\in\mathcal{B}} F_{\mathsf{B}_n}(\xi_n|\boldsymbol{\theta}). \tag{13}$$

Remark 3: In general, a different threshold ξ_i can be used for each bin index i when it is important to account for the variation among the energy samples.

1) Threshold Crossing Search: The TCS algorithm first searches for each bin value b_i that crosses a threshold ξ_i for all

[4]Range estimate and TOA estimate will be used interchangeably owing to the bijective relation between the two.

[5]For brevity, $f_{\mathsf{I}}(i|\boldsymbol{\theta})$ will be used to denote $f_{\mathsf{I}}(i|\mathcal{C}_{\rm th}, \boldsymbol{\theta})$.

$i \in \mathcal{B}$. The algorithm then selects, if $\mathcal{C}_{\text{th}}$ occurs, the bin index $\hat{\imath}$ as the smallest i for which $b_i > \xi_i$. Mathematically,

$$\hat{\imath} \overset{|\mathcal{C}_{\text{th}}}{=} \min\{i \in \mathcal{B} | b_i > \xi_i\}. \tag{14}$$

The PMF of the selected bin index I conditioned on $\mathcal{C}_{\text{th}}$ and $\boldsymbol{\theta}$ is given by (11) with event[6]

$$\mathcal{S}_i \cap \mathcal{C}_{\text{th}} | \boldsymbol{\theta} = \{\mathsf{B}_j \leq \xi_j \, \forall j \in \mathcal{I}_i(i), \mathsf{B}_i > \xi_i | \boldsymbol{\theta}\}. \tag{15}$$

This leads to (16) shown at the bottom of the page. The choice of the thresholds ξ_i's affects the accuracy of the TOA estimation, as well as the detection rate and the false-alarm rate.

2) Maximum Bin Search: The MBS algorithm first searches for the maximum value among all the bins with index $i \in \mathcal{B}$. The algorithm then selects, if $\mathcal{C}_{\text{th}}$ occurs, the bin index $\hat{\imath}$ as the i for which $b_j \leq b_i$ for all $j \neq i$. Mathematically,

$$\hat{\imath} \overset{|\mathcal{C}_{\text{th}}}{=} \underset{i \in \mathcal{B}}{\operatorname{argmax}} \; b_i. \tag{17}$$

The PMF of the selected bin index I conditioned on $\mathcal{C}_{\text{th}}$ and $\boldsymbol{\theta}$ is given by (11) with event

$$\begin{aligned} \mathcal{S}_i \cap \mathcal{C}_{\text{th}} | \boldsymbol{\theta} &= \{i \text{ is selected}, i \text{ is the max}, \mathcal{C}_{\text{th}} | \boldsymbol{\theta}\} \\ &= \{\mathsf{B}_j \leq \mathsf{B}_i \, \forall j \in \mathcal{B} \backslash \{i\} | \boldsymbol{\theta}\} \\ &\quad \backslash \{\mathsf{B}_j \leq \xi_j \, \forall j \in \mathcal{B}, \mathsf{B}_j \leq \mathsf{B}_i \, \forall j \in \mathcal{B} \backslash \{i\} | \boldsymbol{\theta}\}. \end{aligned} \tag{18}$$

[6]The index set $\mathcal{I}_{N_{\text{w}}}(m)$ is defined as $\mathcal{I}_{N_{\text{w}}}(m) = \mathcal{B} \cap \{m - N_{\text{w}}, m - N_{\text{w}} + 1, \ldots, m-1\}$ and its complement over $\mathcal{B}$ as $\mathcal{I}^{\text{c}}_{N_{\text{w}}}(m) = \mathcal{B} \backslash \mathcal{I}_{N_{\text{w}}}(m)$. The set $\mathcal{I}_{N_{\text{w}}}(m)$ is empty for $N_{\text{w}} \leq 0$.

This leads to (19) shown at the bottom of the page, with $\breve{\xi}_j(b) = \min\{\xi_j, b\}$. Note that MBS with thresholds $\xi_j = 0 \, \forall j \in \mathcal{B}$ corresponds to MBS unconditioned on $\mathcal{C}_{\text{th}}$ (i.e., selecting the maximum bin even when none of the bins crosses its threshold). In such a case, (19) degenerates to the PMF of the selected bin index for MBS unconditioned on $\mathcal{C}_{\text{th}}$, which is given by

$$f_{\mathsf{I}}(i|\boldsymbol{\theta}) = \int_0^{+\infty} \prod_{j \in \mathcal{B} \backslash \{i\}} F_{\mathsf{B}_j}(b|\boldsymbol{\theta}) \, f_{\mathsf{B}_i}(b|\boldsymbol{\theta}) \, db.$$

3) Jump Back and Search Forward: The JBSF algorithm first identifies the index m corresponding to the maximum bin value, jumps back to the bin with smallest index in $\mathcal{I}_{N_{\text{w}}}(m)$, and searches forward for each bin value b_i that crosses a threshold ξ_i for all $i \in \mathcal{I}_{N_{\text{w}}}(m)$.[7] The algorithm then selects, if $\mathcal{C}_{\text{th}}$ occurs, the bin index $\hat{\imath}$ as the smallest i for which $b_i > \xi_i$ or as m if none of them crosses the threshold. Mathematically,

$$\hat{\imath} \overset{|\mathcal{C}_{\text{th}}}{=} \min\{\{i \in \mathcal{I}_{N_{\text{w}}}(m) | b_i > \xi_i\} \cup \{m\}\}. \tag{20}$$

The PMF of the selected bin index I conditioned on $\mathcal{C}_{\text{th}}$ and $\boldsymbol{\theta}$ is given by (11) with events

$$\mathcal{S}_i \cap \mathcal{C}_{\text{th}} | \boldsymbol{\theta} = \mathcal{M}_i | \boldsymbol{\theta} \cup \mathcal{M}_i^{\text{c}} | \boldsymbol{\theta} \tag{21a}$$

$$\mathcal{M}_i | \boldsymbol{\theta} = \{i \text{ is selected}, i \text{ is the max}, \mathcal{C}_{\text{th}} | \boldsymbol{\theta}\} \tag{21b}$$

$$\mathcal{M}_i^{\text{c}} | \boldsymbol{\theta} = \{i \text{ is selected}, i \text{ is not the max}, \mathcal{C}_{\text{th}} | \boldsymbol{\theta}\}. \tag{21c}$$

[7]Here N_{w} denotes the window length. For example, the window length N_{w} can be chosen according to the channel delay spread and the transmitted signal.

$$f_{\mathsf{I}}(i|\boldsymbol{\theta}) = \left[1 - F_{\mathsf{B}_i}(\xi_i|\boldsymbol{\theta})\right] \prod_{j \in \mathcal{I}_i(i)} F_{\mathsf{B}_j}(\xi_j|\boldsymbol{\theta}) \left[1 - \prod_{n \in \mathcal{B}} F_{\mathsf{B}_n}(\xi_n|\boldsymbol{\theta})\right]^{-1} \tag{16}$$

$$f_{\mathsf{I}}(i|\boldsymbol{\theta}) = \left[\int_0^{+\infty} \prod_{j \in \mathcal{B} \backslash \{i\}} F_{\mathsf{B}_j}(b|\boldsymbol{\theta}) \, f_{\mathsf{B}_i}(b|\boldsymbol{\theta}) \, db - \int_0^{\xi_i} \prod_{j \in \mathcal{B} \backslash \{i\}} F_{\mathsf{B}_j}(\breve{\xi}_j(b)|\boldsymbol{\theta}) \, f_{\mathsf{B}_i}(b|\boldsymbol{\theta}) \, db\right] \left[1 - \prod_{n \in \mathcal{B}} F_{\mathsf{B}_n}(\xi_n|\boldsymbol{\theta})\right]^{-1} \tag{19}$$

$$\begin{aligned} f_{\mathsf{I}}(i|\boldsymbol{\theta}) = \Bigg[&\int_0^{+\infty} \prod_{j \in \mathcal{I}_{N_{\text{w}}}(i)} F_{\mathsf{B}_j}(\breve{\xi}_j(b)|\boldsymbol{\theta}) \prod_{j \in \mathcal{I}^{\text{c}}_{N_{\text{w}}}(i) \backslash \{i\}} F_{\mathsf{B}_j}(b|\boldsymbol{\theta}) \, f_{\mathsf{B}_i}(b|\boldsymbol{\theta}) \, db - \int_0^{\xi_i} \prod_{j \in \mathcal{B} \backslash \{i\}} F_{\mathsf{B}_j}(\breve{\xi}_j(b)|\boldsymbol{\theta}) \, f_{\mathsf{B}_i}(b|\boldsymbol{\theta}) \, db \\ &+ \sum_{m \in \mathcal{I}_{N_{\text{w}}}(i+N_{\text{w}}+1)} \int_{\xi_i}^{+\infty} \prod_{j \in \mathcal{I}_{i-m+N_{\text{w}}}(i)} F_{\mathsf{B}_j}(\breve{\xi}_j(b)|\boldsymbol{\theta}) [F_{\mathsf{B}_i}(b|\boldsymbol{\theta}) - F_{\mathsf{B}_i}(\xi_i|\boldsymbol{\theta})] \prod_{j \in \mathcal{I}^{\text{c}}_{i-m+N_{\text{w}}}(i) \backslash \{i,m\}} F_{\mathsf{B}_j}(b|\boldsymbol{\theta}) \, f_{\mathsf{B}_m}(b|\boldsymbol{\theta}) \, db\Bigg] \\ &\times \left[1 - \prod_{n \in \mathcal{B}} F_{\mathsf{B}_n}(\xi_n|\boldsymbol{\theta})\right]^{-1} \end{aligned} \tag{23}$$

$$\begin{aligned} f_{\mathsf{I}}(i|\boldsymbol{\theta}) = \Bigg[&\int_0^{+\infty} \breve{F}_{\mathsf{B}_{i-1}}(\breve{\xi}_{i-1}(b)|\boldsymbol{\theta}) \prod_{j \in \mathcal{B} \backslash \{i-1,i\}} F_{\mathsf{B}_j}(b|\boldsymbol{\theta}) f_{\mathsf{B}_i}(b|\boldsymbol{\theta}) \, db - \int_0^{\xi_i} \prod_{j \in \mathcal{B} \backslash \{i\}} F_{\mathsf{B}_j}(\breve{\xi}_j(b)|\boldsymbol{\theta}) \, f_{\mathsf{B}_i}(b|\boldsymbol{\theta}) \, db \\ &+ \sum_{m \in \mathcal{I}_{N_{\text{b}}-i-1}(N_{\text{b}})} \int_{\xi_{m,i}}^{+\infty} \breve{F}_{\mathsf{B}_{i-1}}(\breve{\xi}_{i-1}(b)|\boldsymbol{\theta}) \prod_{j \in \mathcal{I}_{m-i}(m)} [F_{\mathsf{B}_j}(b|\boldsymbol{\theta}) - F_{\mathsf{B}_j}(\xi_j|\boldsymbol{\theta})] \prod_{j \in \mathcal{I}^{\text{c}}_{m-i}(m) \backslash \{i-1,m\}} F_{\mathsf{B}_j}(b|\boldsymbol{\theta}) \, f_{\mathsf{B}_m}(b|\boldsymbol{\theta}) \, db\Bigg] \\ &\times \left[1 - \prod_{n \in \mathcal{B}} F_{\mathsf{B}_n}(\xi_n|\boldsymbol{\theta})\right]^{-1} \end{aligned} \tag{26}$$

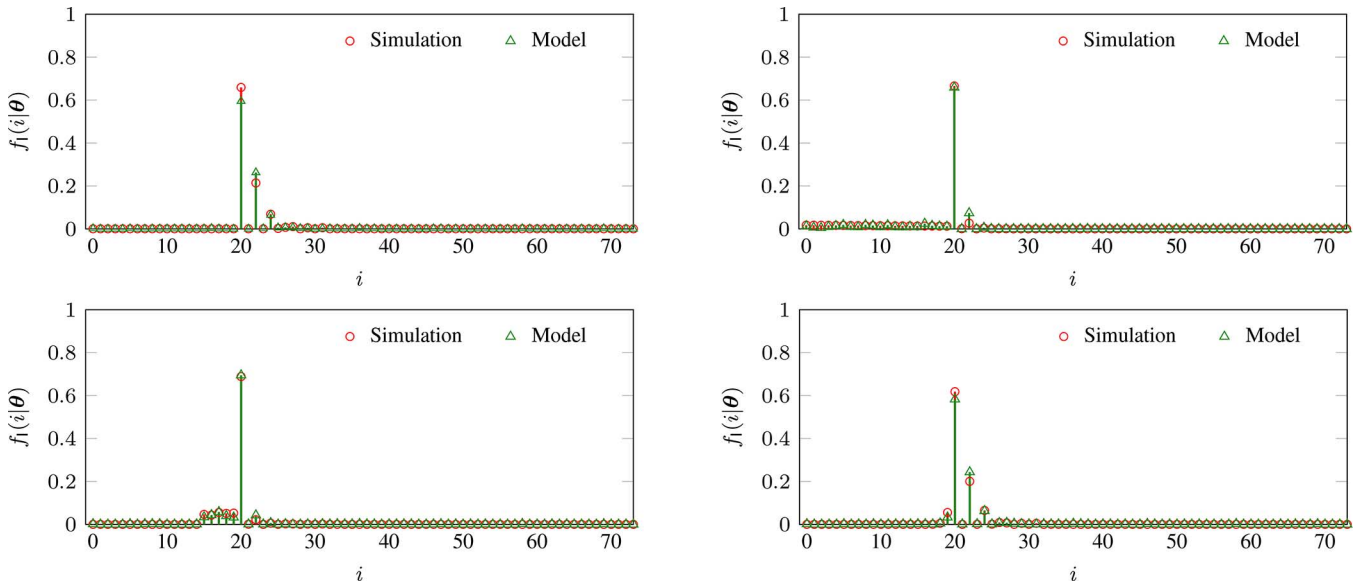

Fig. 2. Example PMF of the selected bin index for the TCS (top left), MBS (top right), JBSF with $N_{\mathrm{w}} = 5$ (bottom left), and SBS (bottom right) algorithms with $T_{\mathrm{d}} = 2$ ns, $N_{\mathrm{p}} = 128$, and $\gamma = -10$ dB. The first bin containing the transmitted signal has index $i = 20$.

In particular,

$$\mathcal{M}_i|\boldsymbol{\theta} = \{\mathsf{B}_j \leq \xi_j \,\forall j \in \mathcal{I}_{N_{\mathrm{w}}}(i), \mathsf{B}_j \leq \mathsf{B}_i \,\forall j \in \mathcal{B}\backslash\{i\}|\boldsymbol{\theta}\} \backslash\{\mathsf{B}_j \leq \xi_j \,\forall j \in \mathcal{B}, \mathsf{B}_j \leq \mathsf{B}_i \,\forall j \in \mathcal{B}\backslash\{i\}|\boldsymbol{\theta}\} \quad (22a)$$

$$\mathcal{M}_i^{\mathrm{c}}|\boldsymbol{\theta} = \bigcup_{m \in \mathcal{I}_{N_{\mathrm{w}}}(i+N_{\mathrm{w}}+1)} \{\mathsf{B}_j \leq \xi_j \,\forall j \in \mathcal{I}_{i-m+N_{\mathrm{w}}}(i), \mathsf{B}_i > \xi_i, \mathsf{B}_j \leq \mathsf{B}_m \,\forall j \in \mathcal{B}\backslash\{m\}|\boldsymbol{\theta}\}. \quad (22b)$$

This leads to (23) shown at the bottom of previous page.[8] Note that JBSF with $N_{\mathrm{w}} = 0$ corresponds to MBS. In such a case, (23) degenerates to (19).

4) Serial Backward Search: The SBS algorithm first identifies the index m corresponding to the maximum bin value, and searches backward for each bin value b_i that crosses a threshold ξ_i for all $i \in \mathcal{I}_m(m)$. The algorithm then selects, if $\mathcal{C}_{\mathrm{th}}$ occurs, the bin index $\hat{\imath}$ as the smallest i for which $b_j > \xi_j$ for all $j \in \mathcal{I}_{m-i}(m)$ or as m if none of them crosses the threshold. Mathematically,

$$\hat{\imath} \overset{|\mathcal{C}_{\mathrm{th}}}{=} \min\{\{i \in \mathcal{I}_m(m) | b_j > \xi_j \,\forall j \in \mathcal{I}_{m-i}(m)\} \cup \{m\}\}. \quad (24)$$

The PMF of the selected bin index I conditioned on $\mathcal{C}_{\mathrm{th}}$ and $\boldsymbol{\theta}$ is given by (11) with the events as in (21). In particular,

$$\mathcal{M}_i|\boldsymbol{\theta} = \{\mathsf{B}_{i-1} \leq \xi_{i-1} \text{ if } i > 0, \mathsf{B}_j \leq \mathsf{B}_i \,\forall j \in \mathcal{B}\backslash\{i\}|\boldsymbol{\theta}\} \backslash\{\mathsf{B}_j \leq \xi_j \,\forall j \in \mathcal{B}, \mathsf{B}_j \leq \mathsf{B}_i \,\forall j \in \mathcal{B}\backslash\{i\}|\boldsymbol{\theta}\} \quad (25a)$$

$$\mathcal{M}_i^{\mathrm{c}}|\boldsymbol{\theta} = \bigcup_{m \in \mathcal{I}_{N_{\mathrm{b}}-i-1}(N_{\mathrm{b}})} \{\mathsf{B}_{i-1} \leq \xi_{i-1} \text{ if } i > 0, \mathsf{B}_j > \xi_j \,\forall j \in \mathcal{I}_{m-i}(m), \mathsf{B}_j \leq \mathsf{B}_m \,\forall j \in \mathcal{B}\backslash\{m\}|\boldsymbol{\theta}\}. \quad (25b)$$

This leads to (26) shown at the bottom of the previous page, with

$$\check{F}_{\mathsf{B}_k}(\cdot|\boldsymbol{\theta}) = \begin{cases} F_{\mathsf{B}_k}(\cdot|\boldsymbol{\theta}) & \text{for } k \in \mathcal{B} \\ 1 & \text{for } k \notin \mathcal{B} \end{cases}$$

and $\check{\xi}_{m,i} = \max\{\xi_j \,\forall j \in \mathcal{I}_{m-i}(m)\}$.

To illustrate how the hard-decision algorithms operate, consider a simple case of $N_{\mathrm{b}} = 8$ bins (i.e., $\mathcal{B} = \{0, 1, \ldots, 7\}$) with a vector of bin instantiations and a vector of thresholds given by

$$\mathbf{b} = [0.8, 1.2, 1.3, 2.3, 2.5, 2.8, 2.4, 1.2]$$
$$\boldsymbol{\xi} = [1.3, 1.1, 0.9, 2.5, 1.4, 2.9, 1.9, 1.4].$$

Note that the threshold crossing event is true (bins with index 1, 2, 4, and 6 cross the corresponding thresholds) and the algorithms select a bin index $\hat{\imath}$ according to (14), (17), (20), and (24). In particular, $\hat{\imath} = 1, 5, 2$, and 4 for TCS, MBS, JBSF with $N_{\mathrm{w}} = 3$, and SBS, respectively.

Remark 4: Recall that the PMF $f_{\mathsf{I}}(i|\boldsymbol{\theta})$ for hard-decision algorithms derived above are conditioned on the threshold crossing event $\mathcal{C}_{\mathrm{th}}$ and $\boldsymbol{\theta}$. Expressions for the joint PMF of I and $\mathcal{C}_{\mathrm{th}}$ conditioned on $\boldsymbol{\theta}$ can be obtained by $\check{f}_{\mathsf{I}}(i|\boldsymbol{\theta}) = f_{\mathsf{I}}(i|\boldsymbol{\theta})[1 - \prod_{n \in \mathcal{B}} F_{\mathsf{B}_n}(\xi_n|\boldsymbol{\theta})]$. The distribution $f_{\mathsf{I}}(i|\boldsymbol{\theta})$ of the selected bin index for numerous other hard-decision algorithms can be derived following a similar approach.

Fig. 2 shows examples of PMF $f_{\mathsf{I}}(i|\boldsymbol{\theta})$ for the TCS, MBS, JBSF with $N_{\mathrm{w}} = 5$, and SBS algorithms with $T_{\mathrm{d}} = 2$ ns, $N_{\mathrm{p}} = 128$, and $\gamma = -10$ dB, according to the IEEE 802.15.4a standard for indoor propagation [57]. It can be observed that the PMF derived based on the proposed range information model are in agreement with those obtained through sample-level simulations (i.e., simulating the wireless channel and the ED operation). In particular, theory and simulations show the same bin index for which the PMF reaches its maximum value.

C. Range Error

We now determine the distribution of the TOA estimation error, which depends on the particular hard-decision algorithm.

[8]The product is equal to 1 and the sum is equal to 0 if evaluated over an empty index set.

The TOA estimation error $e(\tau) = \hat{\tau} - \tau$ is an instantiation of the RV $\mathsf{E} = \mathsf{T} - \tau$, and thus

$$f_{\mathsf{E}}(e|\boldsymbol{\theta}) = f_{\mathsf{T}}(e + \tau|\boldsymbol{\theta}).$$

For a given τ, E belongs to a finite set $\mathcal{E}_\tau = \{\mathsf{T} - \tau \text{ s.t. } \mathsf{T} \in g(\mathcal{B})\}$, where $g(\mathcal{B})$ represents a finite set of TOA estimate. In the absence of a prior information on the true TOA, τ can be modeled as a uniform RV over the interval $[0, T_{\mathrm{a}}]$, where T_{a} is the maximum possible TOA that depends on the wireless environment.[9] Therefore,

$$f_{\mathsf{E}}(e|\boldsymbol{\theta}_{\mathrm{d}}) = \frac{1}{T_{\mathrm{a}}} \int_0^{T_{\mathrm{a}}} f_{\mathsf{E}}(e|\boldsymbol{\theta}_{\mathrm{d}}, \tau)\, d\tau \tag{27}$$

where

$$f_{\mathsf{E}}(e|\boldsymbol{\theta}_{\mathrm{d}}, \tau) = \begin{cases} \left|\frac{d\, g^{-1}(e+\tau)}{d\, e}\right| f_{\mathsf{I}}(g^{-1}(e+\tau)|\boldsymbol{\theta}_{\mathrm{d}}, \tau) & \text{for } e \in \mathcal{E}_\tau \\ 0 & \text{otherwise} \end{cases} \tag{28}$$

with $f_{\mathsf{I}}(i|\boldsymbol{\theta}_{\mathrm{d}}, \tau) = \mathbb{E}_{\boldsymbol{\theta}_{\mathrm{h}}}\{f_{\mathsf{I}}(i|\boldsymbol{\theta})\}$. For specific hard-decision algorithms, (28) can be evaluated by substituting the PDF and CDF of B_i given respectively by (10a) and (10b) into the specific conditional PMF $f_{\mathsf{I}}(i|\boldsymbol{\theta})$ derived in Section III.B and taking the expectation over the vector of noncentrality parameters $\boldsymbol{\lambda} = [\lambda_0, \lambda_1, \ldots, \lambda_{N_{\mathrm{b}}-1}]$.

Remark 5: The distribution of the TOA estimate requires both the evaluation of cumbersome expressions and the expectation over all the channel parameters. This calls for a tractable range information model.

IV. Tractable Range Information Model

The design of soft-decision and hard-decision algorithms demands tractable expressions for the range information model, which can be obtained by simplifying $f_{\mathsf{B}_j}(b|\boldsymbol{\theta})$ and $F_{\mathsf{B}_j}(b|\boldsymbol{\theta})$. First, recall that the chi-squared RV converges in distribution to a Gaussian RV as the number of degrees of freedom increases [58]–[60]. Therefore $\mathsf{B}_i N_{\mathrm{p}}/\sigma^2$ in (8) converges in distribution as

$$\mathsf{B}_i \frac{N_{\mathrm{p}}}{\sigma^2} \xrightarrow{\mathrm{d}} \tilde{\mathsf{B}}_i \frac{N_{\mathrm{p}}}{\sigma^2} \overset{|\boldsymbol{\theta}}{\sim} \mathcal{N}(N_{\mathrm{p}} N_{\mathrm{sb}} + \lambda_i, 2(N_{\mathrm{p}} N_{\mathrm{sb}} + 2\lambda_i)) \tag{29}$$

and consequently

$$f_{\mathsf{B}_i}(b|\boldsymbol{\theta}) \simeq \frac{N_{\mathrm{p}}/\sigma^2}{\sqrt{2(N_{\mathrm{p}} N_{\mathrm{sb}} + 2\lambda_i)}}\, \phi\left(\frac{bN_{\mathrm{p}}/\sigma^2 - N_{\mathrm{p}} N_{\mathrm{sb}} - \lambda_i}{\sqrt{2(N_{\mathrm{p}} N_{\mathrm{sb}} + 2\lambda_i)}}\right) \tag{30}$$

$$F_{\mathsf{B}_i}(b|\boldsymbol{\theta}) \simeq \Phi\left(\frac{bN_{\mathrm{p}}/\sigma^2 - N_{\mathrm{p}} N_{\mathrm{sb}} - \lambda_i}{\sqrt{2(N_{\mathrm{p}} N_{\mathrm{sb}} + 2\lambda_i)}}\right). \tag{31}$$

The above approximation depends on $N_{\mathrm{p}}\, N_{\mathrm{sb}}$ and is accurate for $N_{\mathrm{p}} \gg 1$ or $T_{\mathrm{d}} \gg T_{\mathrm{s}}$. Note that the above distributions depend on the instantiation of the wireless channel through $\boldsymbol{\theta}_{\mathrm{h}}$ in $\boldsymbol{\theta}$. However, the knowledge of the exact channel instantiation is typically not available.

We seek to further simplify the range information model by considering distributions that depend on channel statistics rather than channel instantiations, i.e., on $\bar{\boldsymbol{\theta}} = [\tau\ \bar{\boldsymbol{\theta}}_{\mathrm{h}}\ \boldsymbol{\theta}_{\mathrm{d}}]$ instead of $\boldsymbol{\theta}$, where $\bar{\boldsymbol{\theta}}_{\mathrm{h}}$ represents the channel statistics. Recall that the sample average $\mathsf{X}_n^{(i,s)}$ in (7) depends on $[\tau\ \boldsymbol{\theta}_{\mathrm{h}}\ \boldsymbol{\theta}_{\mathrm{d}}]$ through $\mathsf{U}_{i,p,s}$ and on $\boldsymbol{\theta}_{\mathrm{d}}$ through $\mathsf{N}_{i,p,s}$. Therefore we approximate $\mathsf{X}_n^{(i,s)}$ with $\mathsf{Y}_n^{(i,s)}$ in which $\mathsf{U}_{i,p,s}$ is replaced with a deterministic quantity $U_{i,s}$ that depends on $\bar{\boldsymbol{\theta}}$ as[10]

$$\mathsf{Y}_n^{(i,s)} = \frac{1}{n} \sum_{p=0}^{n-1} (U_{i,s} + \mathsf{N}_{i,p,s})^2. \tag{32}$$

The choice of $U_{i,s}$ is motivated by the following lemma.

Lemma 1: The sample average $\mathsf{Z}_n^{(i,s)} \triangleq \mathsf{X}_n^{(i,s)} - \mathsf{Y}_n^{(i,s)}$ converges almost surely to 0 if and only if $U_{i,s}^2 = \mathbb{E}\{\mathsf{U}^2\}$.

Proof: First note that

$$\mathsf{Z}_n^{(i,s,\nu)} = \frac{1}{n} \sum_{p=0}^{n-1} \left[\mathsf{U}_{i,p,s}^2 - U_{i,s}^2 + 2\mathsf{N}_{i,p,s}(\mathsf{U}_{i,p,s} - U_{i,s})\right].$$

Therefore, as n increases, $\mathsf{Z}_n^{(i,s)}$ converges to $\mathbb{E}\{\mathsf{U}^2\} - U_{i,s}^2$ almost surely by the strong law of large numbers [61]–[63]. Thus, $\mathsf{X}_n^{(i,s)}$ converges almost surely to $\mathsf{Y}_n^{(i,s)}$ if and only if $U_{i,s}^2 = \mathbb{E}\{\mathsf{U}^2\}$. □

Lemma 1 suggests

$$\mathsf{B}_i \simeq \frac{1}{N_{\mathrm{p}}} \sum_{p=0}^{N_{\mathrm{p}}-1} \sum_{s=0}^{N_{\mathrm{sb}}-1} \left(\sqrt{\mathbb{E}\{\mathsf{U}_{i,p,s}^2\}} + \mathsf{N}_{i,p,s}\right)^2 \tag{33}$$

implying that the noncentrality parameter for $\mathsf{B}_i N_{\mathrm{p}}/\sigma^2$ can be written as $\lambda_i \simeq \bar{\lambda}_i$, where

$$\bar{\lambda}_i = \sum_{p=0}^{N_{\mathrm{p}}-1} \sum_{s=0}^{N_{\mathrm{sb}}-1} \frac{\mathbb{E}\{\mathsf{U}_{i,p,s}^2\}}{\sigma^2}. \tag{34}$$

Remark 6: The dependence on wireless channel instantiations can be removed by substituting each noncentrality parameter λ_i, which depends on $\boldsymbol{\theta}$, with its expected value $\bar{\lambda}_i$, which depends on $\bar{\boldsymbol{\theta}}$, in all of the above distributions.

The impulse response of a wideband wireless channel at time t is commonly described by [64]–[68]

$$h(t; \varsigma) = \sum_{l=1}^{L(t)} \alpha_l(t)\, \delta(\varsigma - \tau_l(t)) \tag{35}$$

where $L(t)$ is the number of multipath components, and $\alpha_l(t)$ and $\tau_l(t)$ are the amplitude gain and the arrival time of the lth path, respectively.[11] For a resolvable multipath channel, i.e., the path interarrival time intrinsic to the wireless environment is larger than the temporal duration of the transmitted signal, $\mathbb{E}\{\mathsf{U}_{i,p,s}^2\}$ in (34) can be written as

$$\mathbb{E}\{\mathsf{U}_{i,p,s}^2\} \simeq \mathbb{E}\left\{\sum_{l=1}^{L} \alpha_l^2 s^2(t_{i,p,s} - \tau_l)\right\}. \tag{36}$$

Therefore, the calculation of $\bar{\lambda}_i$ requires the averaging with respect to the channel nuisance parameters α_l's and τ_l's in $\boldsymbol{\theta}_{\mathrm{h}}$.

[9] This results in $\mathcal{E}_\tau = [-T_{\mathrm{a}}, T_{\mathrm{obs}}]$ with, in general, $0 < T_{\mathrm{a}} \leq T_{\mathrm{obs}}$. When the wireless environment is not known, T_{a} can be chosen as $T_{\mathrm{a}} = T_{\mathrm{obs}}$.

[10] A possible choice is $U_{i,s} = \mathbb{E}\{\mathsf{U}^\nu\}^{1/\nu}$, where $\mathbb{E}\{\mathsf{U}^\nu\}$ is the νth order moment of U, which is consistent in terms of the unit measure of $U_{i,s}$ and $\mathsf{N}_{i,p,s}$. Also, $\mathbb{E}\{\mathsf{U}^\nu\}^{1/\nu}$ is monotonically increasing in ν by Lyapunov's inequality.

[11] The $L(t)$, $\alpha_l(t)$, and $\tau_l(t)$ are considered time-invariant over an observation time.

The complexity of such calculation depends on the joint distribution of L, α_l's, and τ_l's. However, the resolution of the ED is limited by the dwell time T_d. Therefore, the statistics of the energy bins can be determined by considering a tapped-delay-line model [68]–[72]. In particular, $h(t;\varsigma)$ can be replaced by $\breve{h}(t;\varsigma)=\sum_{l=1}^{\breve{L}}\breve{\alpha}_l\delta(\varsigma-\breve{\tau}_l)$, where $\breve{L}$ is a deterministic number of path, $\breve{\tau}_l=\tau+l\Delta$ with Δ deterministic, and $\breve{L}\Delta$ is the approximate dispersion of the channel.[12] This results in

$$\mathbb{E}\{\,\mathsf{U}_{i,p,s}^2\,\}\simeq\sum_{l=1}^{\breve{L}}\mathbb{E}\{\,\breve{\alpha}_l^2\,\}s^2(t_{i,p,s}-\breve{\tau}_l). \tag{37}$$

Substituting (37) in (34), the expected value of the noncentrality parameter for the ith bin becomes

$$\bar{\lambda}_i=\sum_{p=0}^{N_\mathrm{p}-1}\sum_{s=0}^{N_\mathrm{sb}-1}\sum_{l=1}^{\breve{L}}\frac{\mathbb{E}\{\breve{\alpha}_l^2\}}{\sigma^2}s^2(t_{i,p,s}-\breve{\tau}_l). \tag{38}$$

Using (38) instead of λ_i in all the above distributions, one can obtain the tractable range information model that depends only on $\bar{\boldsymbol{\theta}}$ instead of $\boldsymbol{\theta}$. For instance, B_i can be approximated by $\bar{\mathsf{B}}_i$ with conditional CDF given by

$$F_{\bar{\mathsf{B}}_i}(b|\bar{\boldsymbol{\theta}})=\Phi\left(\frac{bN_\mathrm{p}/\sigma^2-N_\mathrm{p}N_\mathrm{sb}-\bar{\lambda}_i}{\sqrt{2(N_\mathrm{p}N_\mathrm{sb}+2\bar{\lambda}_i)}}\right) \tag{39}$$

which is obtained from (31) by replacing λ_i with $\bar{\lambda}_i$. Fig. 3 shows the CDF of the energy bin for different numbers of observations and dwell times with received signal-to-noise ratio (SNR) per pulse $\gamma=-20$ dB according to the IEEE 802.15.4a standard for indoor residential line-of-sight (LOS) environments [57]. More details about the scenario will be provided in Section VI.B where the case study is presented. It can be observed that the theoretical CDF of the bin value (39) accurately describes the empirical CDF obtained by sample-level simulations.

Using the results in this section, tractable expressions of the distribution of the TOA estimation error can be derived for hard-decision algorithms. In particular, substituting the PDF and CDF of B_i given respectively by (10a) and (10b) into the conditional PMF $f_\mathsf{I}(i|\boldsymbol{\theta})$ in Section III.B for specific hard-decision algorithms, and replacing each λ_i with $\bar{\lambda}_i$, (28) is simplified into a tractable form.

Remark 7: The parameters $\bar{\lambda}_i$'s depend on $\bar{\boldsymbol{\theta}}_\mathrm{h}$ through $\breve{L}$, the statistics of $\breve{\alpha}_l$, and Δ. The $\bar{\lambda}_i$'s depend on $\boldsymbol{\theta}_\mathrm{d}$ through N_sb and $t_{i,p,s}$, which further depends on T_d, T_p, and T_s.

V. Design of the Energy Detector

This section aims to present the design of energy detection algorithms based on the proposed range information model. Such a model enables us to determine ED parameters (e.g., the choice of the thresholds, window length, and dwell time) according to different optimization criteria and constraints.

[12]For example, Δ can be chosen as the dwell time, the inverse of the bandwidth, or the average interarrival time of the paths.

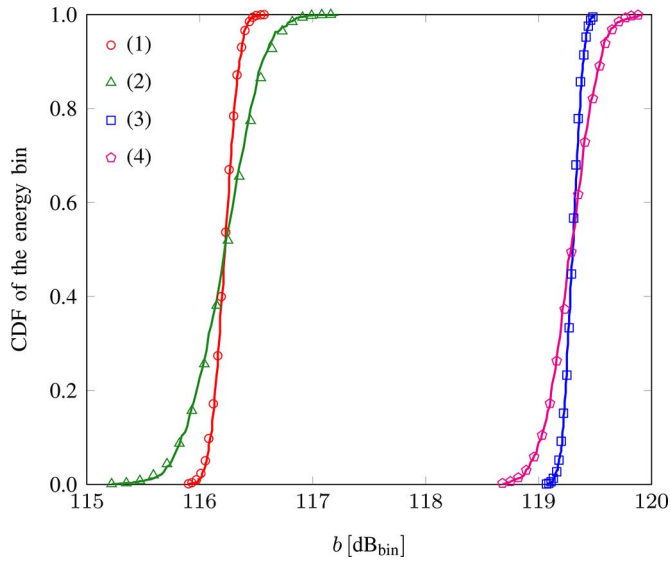

Fig. 3. Example CDF of the energy bin value for different values of N_p and T_d with $\gamma=-20$ dB: (1) $N_\mathrm{p}=128$, $T_\mathrm{d}=2$ ns; (2) $N_\mathrm{p}=16$, $T_\mathrm{d}=2$ ns; (3) $N_\mathrm{p}=128$, $T_\mathrm{d}=4$ ns; (4) $N_\mathrm{p}=16$, $T_\mathrm{d}=4$ ns. Simulation results are shown in symbols and theoretical results according to (39) are shown in solid lines.

The design of ED commonly involves the probability of detection and that of false-alarm. The detection event occurs when, in a presence of the transmitted signal, the presence of the signal is correctly detected. The probability of such an event is given by

$$P_\mathrm{d}(\boldsymbol{\theta}_\mathrm{d})=\sum_{i\in\mathcal{B}}\breve{f}_\mathsf{I}(i|\boldsymbol{\theta}_\mathrm{d},\boldsymbol{\lambda}\neq\mathbf{0}). \tag{40}$$

The false-alarm event occurs when, in an absence of the transmitted signal, the presence of the signal is incorrectly detected due to noise. The probability of such an event is given by

$$P_\mathrm{fa}(\boldsymbol{\theta}_\mathrm{d})=\sum_{i\in\mathcal{B}}\breve{f}_\mathsf{I}(i|\boldsymbol{\theta}_\mathrm{d},\boldsymbol{\lambda}=\mathbf{0}). \tag{41}$$

For a given minimum tolerable level of detection probability $P_\mathrm{d}^\star$ or maximum tolerable level of false-alarm probability $P_\mathrm{fa}^\star$, constraints on parameters value $\boldsymbol{\theta}_\mathrm{d}$ can be obtained.[13]

An important metric for ED design is the mean squared error (MSE) of the TOA estimate. When conditioned on the detection of the transmitted signal, the MSE of the TOA estimate is given by

$$\varrho_\mathrm{t}(\boldsymbol{\theta}_\mathrm{d})=\int_{-\infty}^{+\infty}e^2f_\mathsf{E}(\boldsymbol{\theta}_\mathrm{d})de. \tag{42}$$

Recalling that the TOA estimation error belongs to a finite set $\mathcal{E}_\tau$, the MSE of the TOA estimate for hard-decision algorithms can be written as

$$\varrho_\mathrm{t}(\boldsymbol{\theta}_\mathrm{d})=\frac{1}{T_\mathrm{obs}}\sum_{i=0}^{N_\mathrm{b}-1}\int_0^{T_\mathrm{obs}}(g(i)-\tau)^2f_\mathsf{I}(i|\boldsymbol{\theta}_\mathrm{d},\tau)d\tau. \tag{43}$$

The design of an ED minimizing the MSE of the TOA estimate with a guaranteed minimum level of detection probability

[13]For example, $P_\mathrm{fa}(\boldsymbol{\theta}_\mathrm{d})$ is non-increasing with the threshold ξ and therefore a minimum value ξ_fa can be determined for a given $P_\mathrm{fa}^\star$.

can be obtained by solving the following constrained optimization problem

$$\hat{\boldsymbol{\theta}}_{\mathrm{d}} = \underset{\left\{\boldsymbol{\theta}_{\mathrm{d}} : P_{\mathrm{d}}(\boldsymbol{\theta}_{\mathrm{d}}) \geq P_{\mathrm{d}}^{\star}\right\}}{\operatorname{argmin}} \varrho_{\mathrm{t}}(\boldsymbol{\theta}_{\mathrm{d}}). \tag{44}$$

Instead of guaranteeing a minimum detection probability, the design of an ED can minimize the MSE of the TOA estimate with a guaranteed maximum level of false-alarm probability as

$$\hat{\boldsymbol{\theta}}_{\mathrm{d}} = \underset{\left\{\boldsymbol{\theta}_{\mathrm{d}} : P_{\mathrm{fa}}(\boldsymbol{\theta}_{\mathrm{d}}) \leq P_{\mathrm{fa}}^{\star}\right\}}{\operatorname{argmin}} \varrho_{\mathrm{t}}(\boldsymbol{\theta}_{\mathrm{d}}). \tag{45}$$

The design of an ED can also be formulated to maximize the detection probability $P_{\mathrm{d}}(\boldsymbol{\theta}_{\mathrm{d}})$ for a given maximum tolerable MSE $\varrho_{\mathrm{t}}^{\star}$ of the TOA estimate, i.e.,

$$\hat{\boldsymbol{\theta}}_{\mathrm{d}} = \underset{\left\{\boldsymbol{\theta}_{\mathrm{d}} : \varrho_{\mathrm{t}}(\boldsymbol{\theta}_{\mathrm{d}}) \leq \varrho_{\mathrm{t}}^{\star}\right\}}{\operatorname{argmax}} P_{\mathrm{d}}(\boldsymbol{\theta}_{\mathrm{d}}). \tag{46}$$

Alternatively, the ED design can be based on a hybrid objective function where the optimization problem is formulated to minimize a metric involving the MSE of the TOA estimate and a penalty. The mathematical formulation of such an optimization problem can be written as

$$\hat{\boldsymbol{\theta}}_{\mathrm{d}} = \underset{\boldsymbol{\theta}_{\mathrm{d}}}{\operatorname{argmin}}\, \upsilon_{\mathrm{t}}(\boldsymbol{\theta}_{\mathrm{d}}) \tag{47}$$

where

$$\upsilon_{\mathrm{t}}(\boldsymbol{\theta}_{\mathrm{d}}) = \varrho_{\mathrm{t}}(\boldsymbol{\theta}_{\mathrm{d}})\, P_{\mathrm{d}}(\boldsymbol{\theta}_{\mathrm{d}}) + \nu(\boldsymbol{\theta}_{\mathrm{d}})\, [1 - P_{\mathrm{d}}(\boldsymbol{\theta}_{\mathrm{d}})] \tag{48}$$

is the unconditional MSE of the TOA estimate and $\nu(\boldsymbol{\theta}_{\mathrm{d}})$ is a penalty in an absence of detection.[14]

The above optimization problems are typical examples for the design of a ranging system. However, the proposed range information model is general and can be used to formulate other optimization problems that arise from energy detection applications.

VI. Case Study

This section defines the performance metrics, describes the case study scenario, and presents performance results based on the developed theory and sample-level simulations.

A. Performance Metrics

Performance of the proposed range information model is evaluated in terms of the PMF accuracy, ranging accuracy, and localization accuracy defined as follows.

1) PMF Accuracy: The following metrics will be used as a measure of the distance between the PMF $f_{\mathsf{I}}(i|\boldsymbol{\theta})$ of the selected bin obtained from the proposed range information model and that obtained through sample-level simulations. Let p_1, p_2 be two possible PMF representing a RV taking values on a set $\mathcal{X}$, e.g., one approximate and one exact. The Jensen-Shannon divergence (JSD) is defined as [73]

$$\mathbb{D}_{\mathrm{JS}}\{p_1 p_2\} = \frac{1}{2} \sum_{i \in \mathcal{X}} p_1(i)\, \log\left(\frac{2\, p_1(i)}{p_1(i) + p_2(i)}\right) + \frac{1}{2} \sum_{i \in \mathcal{X}} p_2(i)\, \log\left(\frac{2\, p_2(i)}{p_1(i) + p_2(i)}\right). \tag{49}$$

[14]The penalty $\nu(\boldsymbol{\theta}_{\mathrm{d}})$ can be chosen as a function of the detection probability.

TABLE I
$\mathbb{D}_{\mathrm{JS}}\{p_1, p_2\}$ (Top), $\mathbb{D}_{\mathrm{RMSE}}\{p_1, p_2\}$ (Middle), and $\mathbb{D}_{\mathrm{ME}}\{p_1, p_2\}$ (Bottom) for Theoretical and Simulated PMF of the Selected Bin for Hard-Decision Algorithms

	$N_{\mathrm{p}} = 16$		$N_{\mathrm{p}} = 128$	
	$\gamma = -20$ dB	$\gamma = -10$ dB	$\gamma = -20$ dB	$\gamma = -10$ dB
TCS	0.015	0.013	0.017	0.009
MBS	0.009	0.013	0.010	0.016
JBSF	0.009	0.012	0.010	0.015
SBS	0.009	0.012	0.010	0.015
	$N_{\mathrm{p}} = 16$		$N_{\mathrm{p}} = 128$	
	$\gamma = -20$ dB	$\gamma = -10$ dB	$\gamma = -20$ dB	$\gamma = -10$ dB
TCS	0.006	0.007	0.006	0.011
MBS	0.004	0.006	0.004	0.012
JBSF	0.004	0.006	0.004	0.009
SBS	0.004	0.006	0.004	0.010
	$N_{\mathrm{p}} = 16$		$N_{\mathrm{p}} = 128$	
	$\gamma = -20$ dB	$\gamma = -10$ dB	$\gamma = -20$ dB	$\gamma = -10$ dB
TCS	0.023	0.037	0.028	0.061
MBS	0.010	0.040	0.011	0.089
JBSF	0.010	0.040	0.010	0.054
SBS	0.010	0.038	0.010	0.070

Other important metrics are the root-mean-square error (RMSE), which is defined as

$$\mathbb{D}_{\mathrm{RMSE}}\{p_1, p_2\} = \left[\frac{1}{|\mathcal{X}|} \sum_{i \in \mathcal{X}} |p_1(i) - p_2(i)|^2\right]^{1/2} \tag{50}$$

and the maximum error, which is defined as

$$\mathbb{D}_{\mathrm{ME}}\{p_1, p_2\} = \max_{i \in \mathcal{X}}\{|p_1(i) - p_2(i)|\}. \tag{51}$$

2) Ranging Accuracy: The ranging accuracy is determined in terms of CDF of the TOA estimation error $F_{\mathsf{E}}(e|\boldsymbol{\theta}_{\mathrm{d}})$ and in terms of RMSE of the TOA estimate $\rho_{\mathrm{t}}(\boldsymbol{\theta}_{\mathrm{d}}) = \sqrt{\varrho_{\mathrm{t}}(\boldsymbol{\theta}_{\mathrm{d}})}$. The CDF $F_{\mathsf{E}}(e|\boldsymbol{\theta}_{\mathrm{d}})$ and the RMSE $\rho_{\mathrm{t}}(\boldsymbol{\theta}_{\mathrm{d}})$ are obtained starting from (27) and (42), respectively.

3) Localization Accuracy: The localization accuracy is determined in terms of the localization error outage (LEO). The LEO is defined as the probability that the localization error is above a maximum tolerable value $\epsilon^{\star}$, i.e.,

$$P_{\mathrm{o}}(\boldsymbol{\theta}_{\mathrm{d}}) = \mathbb{E}_{\boldsymbol{\theta}_{\mathrm{h}}}\left\{\mathbb{1}_{(\epsilon^{\star}, +\infty)}\left\{\epsilon(\mathbf{p}|\boldsymbol{\theta})\right\}\right\} \tag{52}$$

where, for a set $\mathcal{A}$,

$$\mathbb{1}_{\mathcal{A}}\{a\} = \begin{cases} 1 & \text{for } a \in \mathcal{A} \\ 0 & \text{otherwise} \end{cases}$$

and $\epsilon(\mathbf{p}|\boldsymbol{\theta}) = \|\hat{\mathbf{p}}(\boldsymbol{\theta}) - \mathbf{p}\|$ is the absolute value of the localization error, in which $\hat{\mathbf{p}}(\boldsymbol{\theta})$ and $\mathbf{p}$ are the estimated position and the true position, respectively.

B. Wireless Scenario and Energy Detector Setting

Consider a network of anchors (nodes with known position) aiming to localize agents (nodes in unknown positions) in an indoor environment. Specifically, the network is composed of

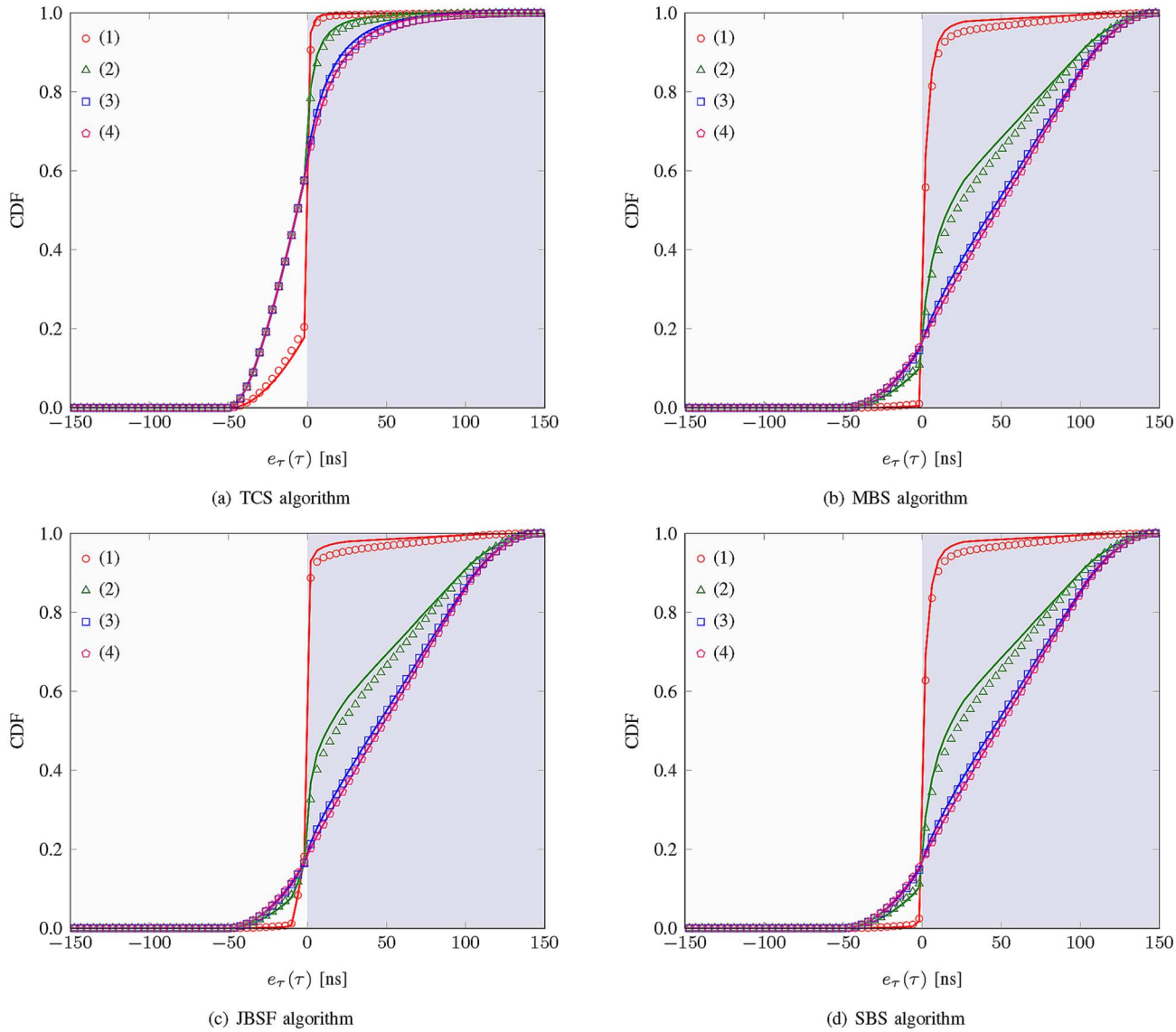

Fig. 4. Example CDF of the TOA estimation error for the TCS, MBS, JBSF with $N_{\mathrm{w}} = 5$, and SBS algorithms with different values of N_{p} and γ: (1) $N_{\mathrm{p}} = 128$, $\gamma = -10$ dB; (2) $N_{\mathrm{p}} = 16$, $\gamma = -10$ dB; (3) $N_{\mathrm{p}} = 128$, $\gamma = -20$ dB; and (4) $N_{\mathrm{p}} = 16$, $\gamma = -20$ dB. Theoretical results are shown in solid lines and simulation results are shown in symbols.

four anchors located at the corners of a square with side length equal to 10 m. Each anchor emits a sequence of ultra-wideband (UWB) root-raised cosine pulses with pulse repetition period $T_{\mathrm{pr}} = 150$ ns. The transmitted power spectral density is compliant with the emission masks according to the following regulations: (a) Japan (Asia Pacific Telecommunity); (b) Europe (European Telecommunications Standards Institute) and Korea (Asia Pacific Telecommunity); (c) USA (Federal Communication Commission); and (d) China (Asia Pacific Telecommunity). The wireless medium follows the IEEE 802.15.4a channel model for UWB indoor residential LOS environments [57] with $T_{\mathrm{a}} = 50$ ns.

The received signal is processed based on energy detection with observation time $T_{\mathrm{obs}} = T_{\mathrm{pr}}$. In the case of hard-decision algorithms, $\xi_i = \xi \, \forall i \in \mathcal{B}$ is considered for illustration.[15] The received SNR per pulse is $\gamma = E_{\mathrm{p}}/N_0$ where E_{p} is the energy of the received signal pulse and N_0 is the one-sided power spectral density (PSD) of the noise component.[16] Unless otherwise stated, the results in the following are provided for an emission mask as defined by the Federal Communication Commission with bandwidth $W = 7.5$ GHz, a number of bins $N_{\mathrm{b}} = 75$, and a dwell time $T_{\mathrm{d}} = 2$ ns. The threshold is chosen according to (44) as the ξ that minimizes the MSE of the TOA estimate with a guaranteed minimum level of detection probability $P_{\mathrm{d}}^{\star} = 95\%$.

[15]The value ξ is commonly chosen by accounting only for the randomness of the noise and discarding that of multipath propagation [74]–[78]. Alternatively, in [20], a simple criterion to determine a threshold is proposed based on the probability of early detection and on the knowledge of noise power. In contrast, the proposed range information model enables us to choose a threshold that accounts for the randomness of the wireless environments.

[16]The noise has mean zero and variance $\sigma^2 = N_0 W$ where W is the bandwidth of the transmitted signal that depends on the emission masks.

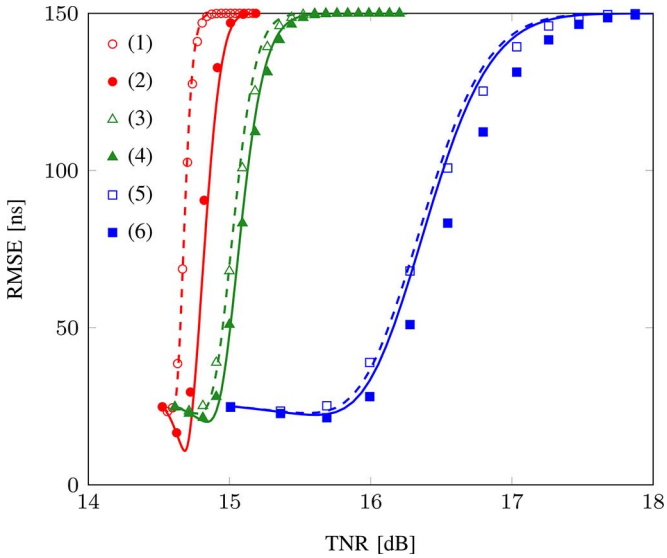

Fig. 5. RMSE of the TOA estimate as a function of TNR per pulse for different values of N_{p} and γ: (1) $N_{\mathrm{p}} = 128$, $\gamma = -20$ dB; (2) $N_{\mathrm{p}} = 128$, $\gamma = -10$ dB; and (3) $N_{\mathrm{p}} = 16$, $\gamma = -20$ dB; (4) $N_{\mathrm{p}} = 16$, $\gamma = -10$ dB; (5) $N_{\mathrm{p}} = 1$, $\gamma = -20$ dB; and (6) $N_{\mathrm{p}} = 1$, $\gamma = -10$ dB. Theoretical results are shown in solid lines and simulation results are shown in symbols.

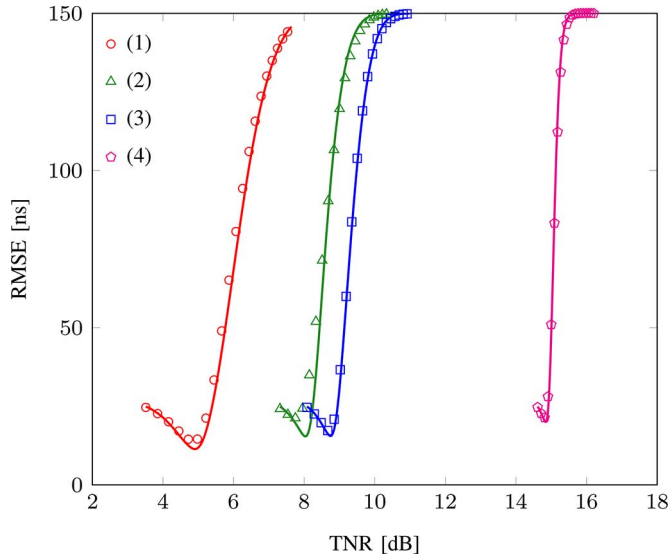

Fig. 6. RMSE of the TOA estimate as a function of TNR per pulse for $N_{\mathrm{p}} = 16$, $\gamma = -10$ dB, and different emission masks: (1) China; (2) Japan; (3) Europe/Korea; and (4) USA. Theoretical results are shown in solid lines and simulation results are shown in symbols.

C. Performance Results

Table I provides the JSD, RMSE, and maximum error between the PMF $f_{\mathrm{I}}(i|\boldsymbol{\theta})$ of the selected bin obtained from the proposed range information model (i.e., (16), (19), (23), or (26)) and that obtained through sample-level simulations for TCS, MBS, JBSF with $N_{\mathrm{w}} = 5$, and SBS algorithms with different values of N_{p} and of γ. It can be noticed that the proposed model for $f_{\mathrm{I}}(i|\boldsymbol{\theta})$ is accurate, having a small distance with respect to the empirical PMF in all the settings.

Fig. 4 shows the CDF of the TOA estimation error (28) for hard-decision algorithms with different values of N_{p} and γ. Two different regions can be discerned for the TOA estimation error: the negative errors (light gray region) due to early detection caused by the noise, and the positive errors (light blue region) due to late detection caused by the wireless channel. It can be observed that the results obtained from the proposed range information model are in agreement with those obtained through sample-level simulations in both regions. It is apparent that the distribution of the TOA estimation error is non Gaussian. Furthermore, the behaviors of the hard-decision algorithms are different in the early detection region, in which the errors are due to false alarms. This behavior is due to the fact that the threshold is chosen to minimize the MSE of the TOA estimate with a guaranteed minimum level of detection probability. Note that, while practical systems typically operate with high N_{p} values, a conservative scenario with small N_{p} values up to 128 is considered here to strain the proposed range information model.

The absolute error of the TOA estimate for $N_{\mathrm{p}} = 128$ and $\gamma = -10$ dB per pulse is evaluated to be below 3.33 ns (corresponding to about 1 m) in 72%, 56%, 73%, and 61% of the instances for TCS, MBS, JBSF with $N_{\mathrm{w}} = 5$, and SBS algorithms, respectively. The absolute error of the TOA estimate is evaluated to be below 5 ns (corresponding to about 1.5 m) in 79%, 79%, 81%, and 80% of the instances for TCS, MBS, JBSF with $N_{\mathrm{w}} = 5$, and SBS algorithms, respectively.

Fig. 5 shows the unconditional RMSE of the TOA estimate for the TCS algorithm as a function of the threshold-to-noise ratio (TNR) per pulse $\xi/(N_{\mathrm{p}}\,\sigma^2)$ for different values of N_{p} and γ. The unconditional RMSE is defined as $\sqrt{v_{\mathrm{t}}(\boldsymbol{\theta}_{\mathrm{d}})}$ where $v_{\mathrm{t}}(\boldsymbol{\theta}_{\mathrm{d}})$ is given in (48) with $\nu(\boldsymbol{\theta}_{\mathrm{d}}) = {T_{\mathrm{obs}}}^2$, which is the maximum possible MSE. It can be seen that the results obtained from the proposed range information model are in agreement with those obtained by sample-level simulations. The accuracy of the proposed model enables us to determine the optimal TNR value that minimizes the RMSE, which is important for ED design. It can also be observed that the minimum RMSE decreases with N_{p} for a given γ. On the other hand, the RMSE varies more rapidly with TNR as N_{p} increases, revealing that the determination of the optimal threshold is critical for large N_{p}.

Fig. 6 shows the unconditional RMSE of the TOA estimate for the TCS algorithm as a function of the TNR per pulse $\xi/(N_{\mathrm{p}}\,\sigma^2)$ for different emission masks, $N_{\mathrm{p}} = 16$, and $\gamma = -10$ dB. In particular, emission masks that are compliant with the regulations of the following countries are considered: (a) China ($W = 0.6$ GHz); (b) Japan ($W = 1.4$ GHz); (c) Europe lower band/Korea ($W = 1.7$ GHz); and (d) USA ($W = 7.5$ GHz). It can be observed that the results obtained from the proposed range information model are in agreement with those obtained through sample-level simulations for all the values of the bandwidth. As shown in Fig. 5, the optimal TNR that minimizes the RMSE can be obtained from the proposed range information model. Note also that the RMSE varies more rapidly as the bandwidth W increases, revealing that the determination of the optimal threshold is critical for large W.

We now determine the localization accuracy of a network in which the agent position is determined according to the maximum likelihood (ML) criterion. In particular, the ML criterion selects the agent position $\hat{\mathbf{p}}$ that maximizes the product of range likelihoods, each in the form of (11) as a function of the TOA corresponding to the relative position between the agent and each anchor. Fig. 7 shows the LEO as a function of the maximum tolerable localization error for soft-decision and hard-decision localization with $T_{\mathrm{d}} = 2$ ns, $N_{\mathrm{p}} = 128$, and different values of the SNR per pulse received at 1 m denoted by γ_0. For hard-decision localization the JBSF algorithm with $N_{\mathrm{w}} = 2$,

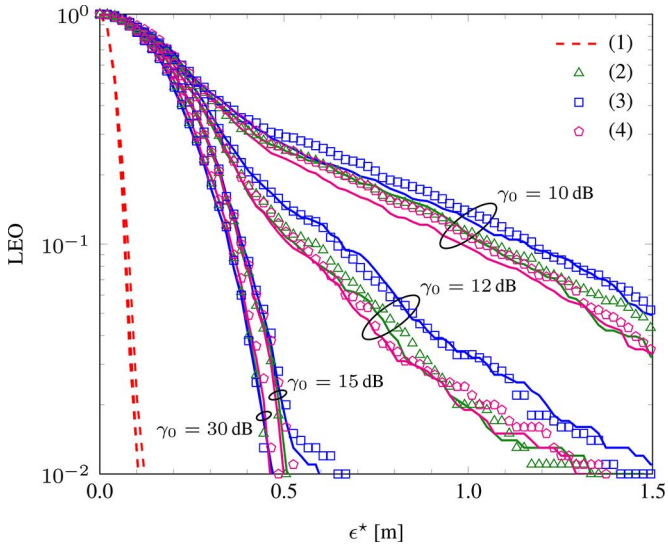

Fig. 7. LEO as a function of the maximum tolerable localization error for soft-decision and hard-decision localization with $T_{\mathrm{d}} = 2$ ns, $N_{\mathrm{p}} = 128$, and different values of γ_0: (1) soft decision (dashed curves from left to right are for γ_0 from 30 to 10 dB); (2) JBSF with $N_{\mathrm{w}} = 5$; (3) JBSF with $N_{\mathrm{w}} = 2$; and (4) TCS. Theoretical results are shown in solid lines and simulation results are shown in symbols.

and 5 as well as the TCS algorithm are considered; the threshold ξ is chosen according to (44) with $P_{\mathrm{d}}^\star = 95\%$. It can be observed that the LEO obtained from the range information model is in agreement with that obtained through sample-level simulations. The effect of N_{w} on the LEO is evident, especially for the smaller γ_0. It can be seen that a localization error smaller than 0.09, 1.45, 1.50, and 1.37 meters can be achieved 95% of the time for case (1), (2), (3), and (4), respectively, with $\gamma_0 = 10$ dB. Similarly, 0.08, 0.39, 0.39, and 0.40 meters can be achieved under the same settings with $\gamma_0 = 30$ dB. The results show that soft-decision localization significantly outperforms hard-decision localization.

VII. Conclusion

A mathematical model for the range information is derived as a function of wireless environment, signal features, and energy detection techniques. Such a model is tractable and serves as a cornerstone for the design and analysis of wideband ranging systems for soft-decision and hard-decision localization. Using the proposed range information model, we have obtained explicit expressions for the range likelihood and range estimate, as well as the distribution of the range estimation error. These expressions form the basis for the design of the energy detector according to a variety of optimization criteria and physical constraints. A case study of a localization network operating in a wireless environment is presented and its performance, in terms of ranging and localization accuracy, is evaluated. The accuracy of the analysis is confirmed by sample-level simulations. The results show that soft-decision localization requiring only the knowledge of channel statistics can significantly outperform hard-decision localization. The proposed range information model provides a new perspective on range-based localization in wireless environments.

Acknowledgment

The authors wish to thank J. C. Allen, N. C. Beaulieu, M. Chiani, R. Cohen, D. Dardari, A. Giorgetti, Y. Shen, and T. Wang for helpful discussions.

References

[1] M. Z. Win, A. Conti, S. Mazuelas, Y. Shen, W. M. Gifford, D. Dardari, and M. Chiani, "Network localization and navigation via cooperation," *IEEE Commun. Mag.*, vol. 49, no. 5, pp. 56–62, May 2011.

[2] N. Patwari, J. N. Ash, S. Kyperountas, A. O. Hero, R. L. Moses, and N. S. Correal, "Locating the nodes: Cooperative localization in wireless sensor networks," *IEEE Signal Process. Mag.*, vol. 22, no. 4, pp. 54–69, July 2005.

[3] K. Pahlavan, X. Li, and J.-P. Mäkelä, "Indoor geolocation science and technology," *IEEE Commun. Mag.*, vol. 40, no. 2, pp. 112–118, Feb. 2002.

[4] J. Hightower and G. Borriello, "Location systems for ubiquitous computing," *Computer*, vol. 34, no. 8, pp. 57–66, Aug. 2001.

[5] Y. Shen and M. Z. Win, "Fundamental limits of wideband localization—Part I: A general framework," *IEEE Trans. Inf. Theory*, vol. 56, no. 10, pp. 4956–4980, Oct. 2010.

[6] Y. Shen, H. Wymeersch, and M. Z. Win, "Fundamental limits of wideband localization—Part II: Cooperative networks," *IEEE Trans. Inf. Theory*, vol. 56, no. 10, pp. 4981–5000, Oct. 2010.

[7] S. Gezici, Z. Tian, G. B. Giannakis, H. Kobayashi, A. F. Molisch, H. V. Poor, and Z. Sahinoglu, "Localization via ultra-wideband radios: A look at positioning aspects for future sensor networks," *IEEE Signal Process. Mag.*, vol. 22, no. 4, pp. 70–84, Jul. 2005.

[8] A. H. Sayed, A. Tarighat, and N. Khajehnouri, "Network-based wireless location: Challenges faced in developing techniques for accurate wireless location information," *IEEE Signal Process. Mag.*, vol. 22, no. 4, pp. 24–40, Jul. 2005.

[9] U. A. Khan, S. Kar, and J. M. F. Moura, "Distributed sensor localization in random environments using minimal number of anchor nodes," *IEEE Trans. Signal Process.*, vol. 57, no. 5, pp. 2000–2016, May 2009.

[10] Y. Shen, S. Mazuelas, and M. Z. Win, "Network navigation: Theory and interpretation," *IEEE J. Sel. Areas Commun.*, vol. 30, no. 9, pp. 1823–1834, Oct. 2012.

[11] U. A. Khan, S. Kar, and J. M. F. Moura, "DILAND: An algorithm for distributed sensor localization with noisy distance measurements," *IEEE Trans. Signal Process.*, vol. 58, no. 3, pp. 1940–1947, Mar. 2010.

[12] D. Dardari, A. Conti, U. J. Ferner, A. Giorgetti, and M. Z. Win, "Ranging with ultrawide bandwidth signals in multipath environments," *Proc. IEEE*, vol. 97, no. 2, pp. 404–426, Feb. 2009.

[13] R. Niu and P. K. Varshney, "Target location estimation in sensor networks with quantized data," *IEEE Trans. Signal Process.*, vol. 54, no. 12, pp. 4519–4528, Dec. 2006.

[14] R. Niu, R. S. Blum, P. K. Varshney, and A. L. Drozd, "Target localization and tracking in noncoherent multiple-input multiple-output radar systems," *IEEE Trans. Aerosp. Electron. Syst.*, vol. 48, no. 2, pp. 1466–1489, Apr. 2012.

[15] M. Arik and O. B. Akan, "Collaborative mobile target imaging in UWB wireless radar sensor networks," *IEEE J. Sel. Areas Commun.*, vol. 28, no. 6, pp. 950–961, Aug. 2010.

[16] S. Bartoletti, A. Conti, A. Giorgetti, and M. Z. Win, "Sensor radar networks for indoor tracking," *IEEE Wireless Commun. Lett.*, vol. 3, no. 2, pp. 157–160, Apr. 2014.

[17] E. Paolini, A. Giorgetti, M. Chiani, R. Minutolo, and M. Montanari, "Localization capability of cooperative anti-intruder radar systems," *EURASIP J. Adv. Signal Process.*, vol. 2008, pp. 1–14, Apr. 2008.

[18] K. K. Mada, H.-C. Wu, and S. S. Iyengar, "Efficient and robust EM algorithm for multiple wideband source localization," *IEEE Trans. Veh. Technol.*, vol. 58, no. 6, pp. 3071–3075, Jul. 2009.

[19] L. Lu, H. Zhang, and H.-C. Wu, "Novel energy-based localization technique for multiple sources," *IEEE Syst. J.*, vol. 8, no. 1, pp. 142–150, Mar. 2014.

[20] D. Dardari, C.-C. Chong, and M. Z. Win, "Threshold-based time-of-arrival estimators in UWB dense multipath channels," *IEEE Trans. Commun.*, vol. 56, no. 8, pp. 1366–1378, Aug. 2008.

[21] L. Stoica, A. Rabbachin, and I. Oppermann, "A low-complexity noncoherent IR-UWB transceiver architecture with TOA estimation," *IEEE Trans. Microw. Theory Tech.*, vol. 54, no. 4, pp. 1637–1646, Jun. 2006.

[22] H. Lu, S. Mazuelas, and M. Z. Win, "Ranging likelihood for wideband wireless localization," in *Proc. IEEE Int. Conf. Commun.*, Budapest, Hungary, Jun. 2013, pp. 4397–4401.

[23] H. Wymeersch, J. Lien, and M. Z. Win, "Cooperative localization in wireless networks," *Proc. IEEE*, vol. 97, no. 2, pp. 427–450, Feb. 2009.

[24] I. Guvenc, C.-C. Chong, F. Watanabe, and H. Inamura, "NLOS identification and weighted least-squares localization for UWB systems using multipath channel statistics," *EURASIP J. Appl. Signal Process.*, vol. 2008, pp. 1–14, 2008, article ID 271984.

[25] S. Maranò, W. M. Gifford, H. Wymeersch, and M. Z. Win, "NLOS identification and mitigation for localization based on UWB experimental data," *IEEE J. Sel. Areas Commun.*, vol. 28, no. 7, pp. 1026–1035, Sep. 2010.

[26] B. Denis and N. Daniele, "NLOS ranging error mitigation in a distributed positioning algorithm for indoor UWB ad-hoc networks," in *Proc. Int. Workshop Wireless Ad-Hoc Netw.*, May/Jun. 2004, pp. 356–360.

[27] S. Venkatesh and R. M. Buehrer, "NLOS mitigation using linear programming in ultrawideband location-aware networks," *IEEE Trans. Veh. Technol.*, vol. 56, no. 5, pp. 3182–3198, Sep. 2007.

[28] A. Conti, M. Guerra, D. Dardari, N. Decarli, and M. Z. Win, "Network experimentation for cooperative localization," *IEEE J. Sel. Areas Commun.*, vol. 30, no. 2, pp. 467–475, Feb. 2012.

[29] A. Conti, D. Dardari, M. Guerra, L. Mucchi, and M. Z. Win, "Experimental characterization of diversity navigation," *IEEE Syst. J.*, vol. 8, no. 1, pp. 115–124, Mar. 2014.

[30] H. Urkowitz, "Energy detection for unknown deterministic signal," *Proc. IEEE*, vol. 55, no. 4, pp. 523–531, Apr. 1967.

[31] C. Xu and C. L. Law, "Delay-dependent threshold selection for UWB TOA estimation," *IEEE Commun. Lett.*, vol. 12, no. 5, pp. 380–382, May 2008.

[32] A. Giorgetti and M. Chiani, "Time-of-arrival estimation based on information theoretic criteria," *IEEE Trans. Signal Process.*, vol. 61, no. 8, pp. 1869–1879, Apr. 2013.

[33] X. Cheng, F. Vanhaverbeke, Y. L. Guan, and M. Moeneclaey, "Blind combining for weighted energy detection of UWB signals," *Electron. Lett.*, vol. 47, no. 1, pp. 55–57, Jan. 2011.

[34] S. Xie, Y. Liu, Y. Zhang, and R. Yu, "A parallel cooperative spectrum sensing in cognitive radio networks," *IEEE Trans. Veh. Technol.*, vol. 59, no. 8, pp. 4079–4092, Oct. 2010.

[35] A. Mariani, A. Giorgetti, and M. Chiani, "Effects of noise power estimation on energy detection for cognitive radio applications," *IEEE Trans. Commun.*, vol. 59, no. 12, pp. 3410–3420, Dec. 2011.

[36] E. Axell, G. Leus, E. G. Larsson, and H. V. Poor, "Spectrum sensing for cognitive radio: State-of-the-art and recent advances," *IEEE Signal Process. Mag.*, vol. 29, no. 3, pp. 101–116, May 2012.

[37] J. W. Chong, D. K. Sung, and Y. Sung, "Cross-layer performance analysis for CSMA/CA protocols: Impact of imperfect sensing," *IEEE Trans. Veh. Technol.*, vol. 59, no. 3, pp. 1100–1108, Mar. 2010.

[38] L. Ye, Z. Zhang, J. Zhang, and H. Zhang, "Carrier sensing with self-cancelation of inter-carrier emission in cognitive OFDMA system," in *Proc. IEEE Int. Conf. Commun.*, Kyoto, Japan, Jun. 2011, pp. 1–6.

[39] I. Ramachandran and S. Roy, "Clear channel assessment in energy-constrained wideband wireless networks," *IEEE Wireless Commun. Mag.*, vol. 14, no. 3, pp. 70–78, Jun. 2007.

[40] N. C. Beaulieu, "Closed-form approximate to PDF of time-average power of bandlimited Gaussian process," *IEE Electron. Lett.*, vol. 32, no. 21, pp. 1948–1950, Oct. 1996.

[41] V. Kostylev, "Energy detection of a signal with random amplitude," in *Proc. IEEE Int. Conf. Commun.*, New York, NY, USA, Apr. 2002, pp. 1606–1610.

[42] J. Salt and H. Nguyen, "Performance prediction for energy detection of unknown signals," *IEEE Trans. Veh. Technol.*, vol. 57, no. 6, pp. 3900–3904, Nov. 2008.

[43] O. Olabiyi and A. Annamalai, "Further results on energy detection of random signals in gaussian noise," in *Proc. IEEE Int. Conf. Connected Veh. Expo*, Las Vegas, NV, USA, Dec. 2013, pp. 14–19.

[44] F. Digham, M.-S. Alouini, and M. K. Simon, "On the energy detection of unknown signals over fading channels," *IEEE Trans. Commun.*, vol. 55, no. 1, pp. 21–24, Jan. 2007.

[45] A. Anttonen, A. Mammela, and A. Kotelba, "Error probability of energy detected multilevel PAM signals in lognormal multipath fading channels," in *Proc. IEEE Int. Conf. Commun.*, Dresden, Germany, Jun. 2009, pp. 1–5.

[46] S. Atapattu, C. Tellambura, and H. Jiang, "Performance of an energy detector over channels with both multipath fading and shadowing," *IEEE Trans. Wireless Commun.*, vol. 9, no. 12, pp. 3662–3670, Dec. 2010.

[47] A. Russ and M. K. Varanasi, "Noncoherent multiuser detection for nonlinear modulation over the Rayleigh-fading channel," *IEEE Trans. Inf. Theory*, vol. 44, no. 1, pp. 295–307, Jan. 2001.

[48] A. Rabbachin, T. Q. Quek, P. C. Pinto, I. Oppermann, and M. Z. Win, "Non-coherent UWB communication in the presence of multiple narrowband interferers," *IEEE Trans. Wireless Commun.*, vol. 9, no. 11, pp. 3365–3379, Nov. 2010.

[49] E. D. Banta, "Energy detection of unknown deterministic signals in the presence of jamming," *IEEE Trans. Aerosp. Electron. Syst.*, vol. AES-14, no. 2, pp. 384–386, Mar. 1978.

[50] N. Patwari, A. O. Hero, III, M. Perkins, N. Correal, and R. O'Dea, "Relative location estimation in wireless sensor networks," *IEEE Trans. Signal Process.*, vol. 51, no. 8, pp. 2137–2148, Aug. 2003.

[51] D. B. Jourdan, D. Dardari, and M. Z. Win, "Position error bound for UWB localization in dense cluttered environments," *IEEE Trans. Aerosp. Electron. Syst.*, vol. 44, no. 2, pp. 613–628, Apr. 2008.

[52] T. Wang, "Cramér-Rao bound for localization with a priori knowledge on biased range measurements," *IEEE Trans. Aerosp. Electron. Syst.*, vol. 48, no. 1, pp. 468–476, Jan. 2012.

[53] J. Shen, A. F. Molisch, and J. Salmi, "Accurate passive location estimation using TOA measurements," *IEEE Trans. Wireless Commun.*, vol. 11, no. 6, pp. 2182–2192, Jun. 2012.

[54] N. Sidiropoulos, A. Swami, and B. Sadler, "Quasi-ML period estimation from incomplete timing data," *IEEE Trans. Signal Process.*, vol. 53, no. 2, pp. 733–739, Feb. 2005.

[55] M. Abramowitz and I. A. Stegun, *Handbook of Mathematical Functions*. New York, NY, USA: Dover, 1970.

[56] I. Guvenc and Z. Sahinoglu, "Threshold-based TOA estimation for impulse radio UWB systems," in *Proc. IEEE Int. Conf. Ultra-Wideband*, Zurich, Switzerland, Sep. 2005, pp. 420–425.

[57] A. F. Molisch, D. Cassioli, C.-C. Chong, S. Emami, A. Fort, B. Kannan, J. Karedal, J. Kunisch, H. Schantz, K. Siwiak, and M. Z. Win, "A comprehensive standardized model for ultrawideband propagation channels," *IEEE Trans. Antennas Propag.*, vol. 54, no. 11, pp. 3151–3166, Nov. 2006.

[58] N. L. Johnson, S. Kotz, and N. Balakrishnan, *Continuous Univariate Distributions*, ser. Wiley Series in Probability and Statistics, 2nd ed. New York, NY, USA: Wiley, 1995, vol. 2.

[59] R. J. Muirhead, *Aspects of Multivariate Statistical Theory*, ser. Wiley Series in Probability and Statistics. Hoboken, NJ: Wiley, 2005.

[60] D. Horgan and C. C. Murphy, "On the convergence of the chi square and noncentral chi square distributions to the normal distribution," *IEEE Commun. Lett.*, vol. 17, no. 12, pp. 2233–2236, Dec. 2013.

[61] I. N. Sanov, "On the probability of large deviations of random variables," *Mat. Sbornik*, vol. 42, pp. 11–44, 1957.

[62] W. Feller, *An Introduction to Probability Theory and Its Applications*. New York, NY, USA: Wiley, 1971, vol. 2.

[63] A. N. Shiryaev, *Probability*, 2nd ed. New York, NY, USA: Springer-Verlag, 1995.

[64] T. Kailath, "Sampling models for linear time-variant filters," Mass. Inst. of Technol., Cambridge, MA, USA, Research Laboratory of Electronics (RLE) Tech. Rep. 352, May 1959.

[65] P. A. Bello, "Characterization of randomly time-variant linear channels," *IEEE Trans. Commun. Syst.*, vol. CS-11, no. 4, pp. 360–393, Dec. 1963.

[66] M. Z. Win and Z. A. Kostić, "Impact of spreading bandwidth on Rake reception in dense multipath channels," *IEEE J. Sel. Areas Commun.*, vol. 17, no. 10, pp. 1794–1806, Oct. 1999.

[67] M. Z. Win, G. Chrisikos, and N. R. Sollenberger, "Performance of Rake reception in dense multipath channels: Implications of spreading bandwidth and selection diversity order," *IEEE J. Sel. Areas Commun.*, vol. 18, no. 8, pp. 1516–1525, Aug. 2000.

[68] J. D. Parsons, *The Mobile Radio Propagation Channel*, 2nd ed. New York, NY, USA: Wiley, 2000.

[69] A. F. Molisch, *Wireless Communications*, 2nd ed. New York, NY, USA: IEEE Press, Wiley, 2010.

[70] A. F. Molisch, L. J. Greenstein, and M. Shafi, "Propagation issues for cognitive radio," *Proc. IEEE*, vol. 97, no. 5, pp. 787–804, May 2009.

[71] H. Hashemi, "The indoor radio propagation channel," *Proc. IEEE*, vol. 81, no. 7, pp. 943–968, Jul. 1993.

[72] D. Cassioli, M. Z. Win, and A. F. Molisch, "The ultra-wide bandwidth indoor channel: From statistical model to simulations," *IEEE J. Sel. Areas Commun.*, vol. 20, no. 6, pp. 1247–1257, Aug. 2002.

[73] J. Lin, "Divergence measures based on the Shannon entropy," *IEEE Trans. Inf. Theory*, vol. 37, no. 1, pp. 145–151, 1991.

[74] A. Maali, A. Mesloub, M. Djeddou, H. Mimoun, G. Baudoin, and A. Ouldali, "Adaptive CA-CFAR threshold for non-coherent IR-UWB energy detector receivers," *IEEE Commun. Lett.*, vol. 13, no. 12, pp. 959–961, Dec. 2009.

[75] Z. Irahhauten, G. Leus, H. Nikookar, and G. Janssen, "UWB ranging based on partial received sub-band signals in dense multipath environments," in *Proc. IEEE Int. Conf. Commun.*, Cape Town, South Africa, May 2010, pp. 1–6.
[76] I. Guvenc and Z. Sahinoglu, "TOA estimation with different IR-UWB transceiver types," in *Proc. IEEE Int. Conf. Ultra-Wideband*, Zurich, Switzerland, Sep. 2005, pp. 426–431.
[77] J.-Y. Lee and R. A. Scholtz, "Ranging in a dense multipath environment using an UWB radio link," *IEEE J. Sel. Areas Commun.*, vol. 20, no. 9, pp. 1677–1683, Dec. 2002.
[78] R. A. Scholtz and J.-Y. Lee, "Problems in modeling UWB channels," *Electron. Lett.*, vol. 20, no. 9, pp. 1–10, Dec. 2002.

Stefania Bartoletti (S'12) received the Laurea degree (*summa cum laude*) in electronics and telecommunications engineering from the University of Ferrara, Italy, in 2011.

Since 2010 she has been a Research Collaborator in the Wireless Communication and Localization Network Laboratory at the University of Ferrara, where she is currently pursuing the Ph.D. degree. Her research interests include theory and experimentation of passive localization and tracking networks, especially with application to wireless sensor radar and RFID systems. From September 2013 to August 2014, she was a visiting Ph.D. student at the Laboratory for Information and Decision Systems, Massachusetts Institute of Technology.

Ms. Bartoletti served as a member of the local organization committee for the 2011 IEEE International Conference on Ultra Wideband (ICUWB) and as a reviewer for numerous IEEE Journals and international Conferences.

Wenhan Dai (S'12) received the B.S. degrees in electronic engineering and in mathematics from Tsinghua University, China, in 2011, and received the S.M. degree in aeronautics and astronautics from the Massachusetts Institute of Technology (MIT), USA, in 2014.

Since 2011, he has been a Research Assistant at the Wireless Communications and Network Science Laboratory, MIT, where he is currently pursuing the Ph.D. degree. His research interests include communication theory, stochastic optimization, and their application to wireless communication and network localization. His current research focuses on resource allocation for network localization, cooperative network operation, and ultra-wide bandwidth communications.

Mr. Dai served as a reviewer for numerous IEEE Journals and international Conferences. He received the academic excellence scholarships from 2008 to 2010 and the Outstanding Thesis Award in 2011 from Tsinghua University.

Andrea Conti (S'99–M'01–SM'11) received the Laurea (*summa cum laude*) in telecommunications engineering and the Ph.D. in electronic engineering and computer science from the University of Bologna, Italy, in 1997 and 2001, respectively.

He is an Associate Professor at the University of Ferrara, Italy. Prior to joining the University of Ferrara, he was with the CNIT and with the IEIIT-Bo of CNR. In Summer 2001, he was with the Wireless Systems Research Department at AT&T Research Laboratories. Since 2003, he has been a frequent visitor to the WCNSL at the Massachusetts Institute of Technology, where he presently holds the Research Affiliate appointment. His research interests involve theory and experimentation of wireless systems and networks including network localization, adaptive diversity communications, cooperative relaying techniques, and network secrecy. He is recipient of the HTE Puskás Tivadar Medal and co-recipient of the IEEE Communications Society's Stephen O. Rice Prize and the IEEE Communications Society's Fred W. Ellersick Prize.

Dr. Conti has served as editor for IEEE journals, as well as organized and chaired numerous international conferences over the last decade. He is elected Chair of the IEEE Communications Society's Radio Communications Technical Committee. He is an elected Fellow of the IET and has been selected as an IEEE Distinguished Lecturer.

Moe Z. Win (S'85–M'87–SM'97–F'04) received both the Ph.D. in electrical engineering and the M.S. in applied mathematics as a Presidential Fellow at the University of Southern California (USC) in 1998. He received the M.S. in electrical engineering from USC in 1989 and the B.S. (*magna cum laude*) in electrical engineering from Texas A&M University in 1987.

He is a Professor at the Massachusetts Institute of Technology (MIT) and the founding director of the Wireless Communication and Network Sciences Laboratory. Prior to joining MIT, he was with AT&T Research Laboratories for five years and with the Jet Propulsion Laboratory for seven years. His research encompasses fundamental theories, algorithm design, and experimentation for a broad range of real-world problems. His current research topics include network localization and navigation, network interference exploitation, intrinsic wireless secrecy, adaptive diversity techniques, and ultra-wide bandwidth systems.

Dr. Win is an elected Fellow of the AAAS, the IEEE, and the IET, and was an IEEE Distinguished Lecturer. He was honored with two IEEE Technical Field Awards: the IEEE Kiyo Tomiyasu Award (2011) and the IEEE Eric E. Sumner Award (2006, jointly with R. A. Scholtz). Together with students and colleagues, his papers have received numerous awards, including the IEEE Communications Society's Stephen O. Rice Prize (2012) and the IEEE Aerospace and Electronic Systems Society's M. Barry Carlton Award (2011). Other recognitions include the International Prize for Communications Cristoforo Colombo (2013), the *Laurea Honoris Causa* from the University of Ferrara (2008), the Technical Recognition Award of the IEEE ComSoc Radio Communications Committee (2008), and the U.S. Presidential Early Career Award for Scientists and Engineers (2004). He was an elected Member-at-Large on the IEEE Communications Society Board of Governors (2011–2013). He was the Chair (2004–2006) and Secretary (2002–2004) for the Radio Communications Committee of the IEEE Communications Society. Over the last two decades, he has served as editor and area editor for IEEE journals, as well as organized and chaired numerous international conferences.